



01 Jun 2006

Calibration of the CoreLok Method for Determination of Missouri Aggregate Specific Gravities

David Newton Richardson

Missouri University of Science and Technology, richardd@mst.edu

S. M. Lusher

Follow this and additional works at: https://scholarsmine.mst.edu/civarc_enveng_facwork



Part of the [Civil Engineering Commons](#)

Recommended Citation

D. N. Richardson and S. M. Lusher, "Calibration of the CoreLok Method for Determination of Missouri Aggregate Specific Gravities," Missouri Department of Transportation (MoDOT), Jun 2006.

This Technical Report is brought to you for free and open access by Scholars' Mine. It has been accepted for inclusion in Civil, Architectural and Environmental Engineering Faculty Research & Creative Works by an authorized administrator of Scholars' Mine. This work is protected by U. S. Copyright Law. Unauthorized use including reproduction for redistribution requires the permission of the copyright holder. For more information, please contact scholarsmine@mst.edu.

Organizational Results Research Report

June 2005

OR06.016

**Calibration of the CoreLok Method for
Determination of Missouri Aggregate Specific
Gravities**

Prepared by Missouri
Transportation Institute and
Missouri Department of
Transportation

Final Report

RI06-017

**Calibration of the CoreLok Method for
Determination of Missouri Aggregate Specific Gravities**

Prepared for

Missouri Department of Transportation
Construction and Materials

By

David N. Richardson, P.E.
Steven M. Lusher, E.I.T.
University of Missouri-Rolla

June 2006

The opinions, findings, and conclusions expressed in this report are those of the principal investigator and the Missouri Department of Transportation. This report does not constitute a standard, specification, or regulation.

TECHNICAL REPORT DOCUMENTATION PAGE

| | | | |
|---|--|--|-----------|
| 1. Report No. OR06-016 | 2. Government Accession No. | 3. Recipient's Catalog No. | |
| 4. Title and Subtitle Calibration of the CoreLok Method for Determination of Missouri Aggregate Specific Gravities | | 5. Report Date June 2006 | |
| | | 6. Performing Organization Code | |
| 7. Author(s) David N. Richardson, Steven M. Lusher | | 8. Performing Organization Report No. | |
| 9. Performing Organization Name and Address Missouri Transportation Institute 710 University Drive Rolla, Missouri 65409 | | 10. Work Unit No. | |
| | | 11. Contract or Grant No. RI06-017 | |
| 12. Sponsoring Agency Name and Address Missouri Department of Transportation Organizational Results P. O. Box 270-Jefferson City, MO 65102 | | 13. Type of Report and Period Covered Final Report | |
| | | 14. Sponsoring Agency Code MoDOT | |
| 15. Supplementary Notes The investigation was conducted in cooperation with the U. S. Department of Transportation, Federal Highway Administration. | | | |
| 16. Abstract Specific gravity and absorption are fundamental aggregate properties needed for hot-mix asphalt (HMA) and Portland cement concrete (PCC) mix design and/or volumetric determinations. MoDOT utilizes the American Association of State Highway and Transportation Officials (AASHTO) standard test methods T 84 (for fine aggregates) and T 85 (for coarse aggregates) to determine these important properties. Criticisms of these procedures are the subjective nature of determining when the aggregates have reached the saturated, surface-dry (SSD) condition (especially T 84) and the substantial amount of time needed to complete the tests. The CoreLok method addresses these criticisms in that it is an objective and faster method for determining aggregate specific gravities. Oven-drying the aggregates to a constant mass is the only sample preparation necessary; there is no need to soak the aggregates for an extended period of time or to obtain the SSD condition in order to complete the test. Apart from sample preparation, the two-part test procedure takes approximately 30 minutes. However, working with dry aggregate poses its own problems and errors are introduced. Therefore to account for these errors, regression analyses were performed to calibrate or "correct" the CoreLok method test results to associated T 84/85 values. | | | |
| 17. Key Words CoreLok, aggregate analysis, specific gravity | | 18. Distribution Statement No restrictions. This document is available to the public through National Technical Information Center, Springfield, Virginia 22161 | |
| 19. Security Classification (of this report) Unclassified | 20. Security Classification (of this page) Unclassified | 21. No. of Pages 37 | 22. Price |

ACKNOWLEDGEMENTS

The authors wish to thank the Missouri Department of Transportation (MoDOT) for sponsoring this work, and in particular, Joe Schroer for supplying and qualifying the data, and giving guidance on implementation of the results. Acknowledgement is also due Ali Regimand (President of InstroTek, Inc., manufacturer of the CoreLok device) for supplying insight into the methodology behind the CoreLok procedure and some earlier attempts at calibration.

EXECUTIVE SUMMARY

Specific gravity and absorption are fundamental aggregate properties needed for hot-mix asphalt (HMA) and Portland cement concrete (PCC) mix design and/or volumetric determinations. MoDOT utilizes the American Association of State Highway and Transportation Officials (AASHTO) standard test methods T 84 (for fine aggregates) and T 85 (for coarse aggregates) to determine these important properties. Criticisms of these procedures are the subjective nature of determining when the aggregates have reached the saturated, surface-dry (SSD) condition (especially T 84) and the substantial amount of time needed to complete the tests.

The CoreLok method addresses these criticisms in that it is an objective and faster method for determining aggregate specific gravities. Oven-drying the aggregates to a constant mass is the only sample preparation necessary; there is no need to soak the aggregates for an extended period of time or to obtain the SSD condition in order to complete the test. Apart from sample preparation, the two-part test procedure takes approximately 30 minutes. However, working with dry aggregate poses its own problems and errors are introduced. Therefore to account for these errors, regression analyses were performed to calibrate or “correct” the CoreLok method test results to associated T 84/85 values.

Conclusions

- The following associated aggregate properties are listed in order of decreasing correlation. The ranking is consistent with AASHTO and American Society for Testing and Materials (ASTM) single-operator precision statements for the standard test method results.
 - Non-corrected CoreLok apparent specific gravity (CorGsa) and T 84/85 apparent specific gravity (Gsa)
 - Non-corrected CoreLok bulk specific gravity (CorGsb) and T 84/85 bulk specific gravity (Gsb).
 - Non-corrected CoreLok absorption (CorABS) and T 84/85 absorption (ABS).
- The recommended G_{sa_pred} (i.e. corrected CorGsa) model is a function of CorGsa and CorABS; i.e. the calculated absorption based on CorGsa and CorGsb [$R^2_{pred} = 0.9641$].
- The recommended G_{sb_pred} (i.e. corrected CorGsb) model is a function of CorGsb and ABS [$R^2_{pred} = 0.9598$]. If ABS is not available, $G_{sb_pred-alt}$ can be obtained using CorABS [$R^2_{pred} = 0.9047$].
- The recommended ABS_{pred} (i.e. corrected CorABS) model is a function of G_{sa_pred} and G_{sb_pred} [$R^2_{pred} = 0.9412$]. Alternatively, $ABS_{pred-alt} = f(G_{sa_pred}, G_{sb_pred-alt})$ [$R^2_{pred} = 0.5007$].
- A secondary analysis suggests that the aggregate durability tests Micro-Deval and Los Angeles Abrasion have statistically significant correlations to Gsb and ABS with Micro-Deval being the more significant of the two.
- Caution is recommended when applying the predictive models to high specific gravity aggregates ($G_{sa} > 2.900$) such as porphyry and steel slag.

TABLE OF CONTENTS

| | Page |
|---|------|
| ACKNOWLEDGEMENTS | iii |
| EXECUTIVE SUMMARY | iii |
| LIST OF ILLUSTRATIONS | v |
| LIST OF TABLES..... | vi |
| INTRODUCTION | 1 |
| Standard Test Methods..... | 1 |
| CoreLok Method | 2 |
| Current Calibration Methods | 3 |
| Objective..... | 4 |
| INVESTIGATION | 5 |
| Data Compilation/Organization | 5 |
| Overall Dataset Modification | 6 |
| Statistical Analysis Methodology..... | 7 |
| Secondary Analyses | 8 |
| RESULTS AND DISCUSSION | 9 |
| Variable Correlations and Comparative Analyses..... | 9 |
| Predictive Models | 13 |
| Apparent Specific Gravity: Gsa | 13 |
| Bulk Specific Gravity: Gsb..... | 14 |
| Absorption: ABS..... | 16 |
| Alternate Bulk Specific Gravity Prediction | 17 |
| Model Validation | 18 |
| Secondary Analysis: Micro-Deval and Los Angeles Abrasion..... | 21 |
| CONCLUSIONS..... | 23 |
| IMPLEMENTATION | 23 |
| SUGGESTED FOLLOW-UP WORK | 24 |

LIST OF ILLUSTRATIONS

| Figure | Page |
|---|------|
| Figure 1: Histogram of Differences: $G_{sb} - CorG_{sb}$ | 11 |
| Figure 2: Histogram of Differences: $G_{sa} - CorG_{sa}$ | 12 |
| Figure 3: Histogram of Differences: $ABS - CorABS$ | 12 |
| Figure 4: Predicted vs. Measured T 84/85 Apparent Specific Gravity..... | 14 |
| Figure 5: Predicted vs. Measured T 84/85 Bulk Specific Gravity | 15 |
| Figure 6: Histogram of Differences: $ABS - ABS_{pred}$ | 16 |
| Figure 7: Predicted vs. Measured T 84/85 Absorption | 17 |
| Figure 8: Predicted (Alternate) vs. Measured T 84/85 Bulk Specific Gravity..... | 18 |
| Figure 9: Model Validation: $G_{sa_{pred}}$ vs. T 84/85 G_{sa} | 19 |
| Figure 10: Model Validation: $G_{sb_{pred}}$ vs. T 84/85 G_{sb} | 20 |
| Figure 11: Model Validation: ABS_{pred} vs. T 84/85 ABS | 20 |

LIST OF TABLES

| Table | Page |
|---|------|
| Table 1: Correlation Matrix..... | 9 |
| Table 2: Paired T-Test Results | 10 |
| Table 3: Correlation Matrix: Micro-Deval & Los Angeles Abrasion as Variables..... | 21 |
| Table 4: 180 Sample Dataset Part 1 | 26 |
| Table 5: 180 Sample Dataset Part 2..... | 27 |
| Table 6: 180 Sample Dataset Part 3..... | 28 |
| Table 7: T 84/85 & Predicted Values Part 1..... | 29 |
| Table 8: T 84/85 & Predicted Values Part 2..... | 30 |
| Table 9: T 84/85 & Predicted Values Part 3..... | 31 |

INTRODUCTION

Specific gravity and absorption are fundamental aggregate properties needed for hot-mix asphalt (HMA) and Portland cement concrete (PCC) mix design and/or volumetric determinations. The definition of specific gravity can be given as the ratio of the mass of a given volume of aggregate to the mass of an equal volume of water at a stated temperature. Absorption can be defined as the mass of water entering the permeable voids of aggregate during submergence in water over a prescribed period of time, but no free water on particle surfaces, expressed as a percentage of the mass of the solids. There are three basic variations of specific gravity. The generic equations used to calculate these three specific gravities and absorption are as follows:

$$G_{sa} = \frac{M_s}{(V_s)\gamma_w} \quad (1)$$

Where: G_{sa} = Apparent specific gravity
 M_s = Mass of the solids (gm)
 V_s = Volume of the solids (cm³)
 γ_w = Density of water (gm/cm³)

$$G_{sb}(OD) = \frac{M_s}{(V_s + V_v)\gamma_w} \quad (2)$$

Where: $G_{sb}(OD)$ = Bulk specific gravity, Oven-Dry basis
 V_v = Volume of water-permeable and impermeable voids within aggregate particles (cm³)

$$G_{sb}(SSD) = \frac{M_s + M_w}{(V_s + V_v)\gamma_w} \quad (3)$$

Where: $G_{sb}(SSD)$ = Bulk specific gravity, Saturated Surface-Dry basis
 M_w = Mass of water absorbed into permeable voids by soaking for prescribed time period but no free water on particle surfaces (gm)

$$ABS = \frac{M_w}{M_s} \times 100\% \quad (4)$$

Where: ABS = Absorption (%)

Standard Test Methods

The Missouri Department of Transportation (MoDOT) utilizes the American Association of State Highway and Transportation Officials (AASHTO) standard test methods T 84, "Specific Gravity and Absorption of Fine Aggregate," and T 85, "Specific Gravity and Absorption of Coarse Aggregate," to determine these important properties. Method T 84 is applied to fine aggregates or those finer than the #4 sieve (4.75 mm mesh) while T 85 is for coarse aggregates or those larger than the #4 sieve. Both test methods follow the same basic procedure in that the aggregates are first oven-dried to a constant mass then submerged in water for a specified length of time. At the end of this time period, the aggregates are brought to the SSD condition through air-drying under T 84 or towel-drying under T

85. This portion of test is the most controversial in that one's judgment must be used to an extent to determine when the free surface water has been removed yet saturation or full absorption has been maintained.

Especially troublesome is the T 84 test method's guidance on determining the SSD condition of fine aggregates. The primary method for ascertaining when the SSD condition has been met is called the cone test. It is a small-scale slump test that indicates when the apparent cohesion caused by surface moisture on the aggregate particles has been reduced such that the fine aggregate is free to flow or "slump." This system works fairly well when the fine aggregate is a natural sand or other material that is somewhat smooth-surfaced, rounded, and relatively free of fines. However, the trend toward using manufactured sands is rapidly increasing and these fine aggregates pose a problem under T 84 in that they do not readily slump in the cone test. There are at least four alternate criteria in T 84 that one can use to determine the SSD condition for these types of materials.

Once the SSD condition is met, SSD weights are determined and the volume-displacement portion of the test methods proceeds through the use of volumetric flasks under T 84 or by weighing while submerged in water under T 85. The final step is to once again oven-dry the test sample to a constant mass and record that weight. Although alternative processes are allowed within T 84 and T 85 to speed the process, the procedure as outlined here is the most commonly used and can take approximately 24 hours (15 for soaking, 8 for all oven-drying, and 1 for the remaining work) or 2 working days to complete. Thus, criticisms of these procedures are the subjective nature of determining when the aggregates have reached the SSD condition (especially T 84) and the substantial amount of time needed to complete the tests.

CoreLok Method

The CoreLok method addresses these criticisms in that it is an objective and faster method for determining aggregate specific gravities. Oven-drying the aggregates to a constant mass is the only sample preparation necessary; there is no need to soak the aggregates for an extended period of time or to obtain the SSD condition in order to complete the test. Apart from sample preparation, the two-part test procedure takes approximately 30 minutes.

One part of the procedure involves using a pycnometer (metal volumeter) to determine Gsb (OD). Please note that throughout the remainder of this paper, Gsb (OD) as defined in Equation 2 will be referred to as simply Gsb when determined using T 84/85 and CorGsb when determined using the CoreLok method. The basic process is identical to the weighing-in-air procedure specified in AASHTO T 209, "Theoretical Maximum Specific Gravity and Density of Bituminous Paving Mixtures." Three weights are required: weight of the oven-dry sample, weight of the pycnometer filled with water, and combined weight of the pycnometer, water, and sample. The major problem with the CorGsb portion of the CoreLok method is that an assumption is made that the oven-dry aggregate absorbs an insignificant amount of water when introduced into the pycnometer. This assumption is enforced within the test procedure by specifying that one has no more than two minutes to finalize the filling of the pycnometer once the aggregate comes into contact with the water. However, the type of material being tested in this manner has an impact on the validity of the assumption. Absorption may be considered a function of two separate properties: rate of absorption and absorptive capacity. Testing an aggregate with a low rate of absorption (despite the capacity) or testing an aggregate with a low absorptive capacity (despite the rate) may work fairly well under the assumption in question. However, it seems prudent to assume the opposite, that there is a significant amount of water taken into the permeable voids of the aggregate during the two minute time period and this ingress of water does affect the results.

The second part of the CoreLok method involves the use of a vacuum chamber to determine Gsa. Again as with Gsb, Gsa will be referred to as CorGsa throughout the remainder of this paper if it pertains to that property determined using the CoreLok method. It is from this device that the method draws its name. The CoreLok device was originally developed by Instrotek, Inc. to perform bulk specific gravity tests on HMA cores or compacted samples and maximum specific gravity tests on HMA loose mix. In fact, there are ASTM standard test methods published for these two procedures. In this portion of the CoreLok method, a second oven-dry sample of the same material tested to determine CorGsb is vacuum sealed within a plastic bag. Once evacuated and sealed, the bag (plus an added bag and protective rubber sheets if coarse aggregate is being tested) is submerged in a water tank set up as a weigh-in-water system. The bag is then opened under water to allow the full and rapid saturation of the aggregate. After a specified amount of time has elapsed, the weight of the bagged sample submerged in water is determined. Knowing the oven-dry weight of the sample, weight and specific gravity of the bag(s) (and rubber sheets if used), and the submerged weight of the bagged sample, one can calculate CorGsa.

The CorGsa determination is not as problematic as the CorGsb portion of the test. However, there are aspects of the CorGsa process that may introduce errors, relative to the standard T 84/85 methods. The magnitude and duration of vacuum application, and the aggregate gradation may affect CorGsa values due to the effect these factors may have on the mechanism with which water is introduced into the permeable voids of the aggregate.

Current Calibration Methods

It is not as if these issues have never been considered. Accounting for the differences between CorGsb and Gsb, and CorGsa and Gsa has been attempted by Instrotek through the embedment of calibration or “corrective” equations into the spreadsheets used in conjunction with the CoreLok method for determining CorGsb and CorGsa. In the AggSpec software that was standard issue with the CoreLok device in 2002, the corrections were applied only to the CorGsb values determined for fine aggregates. This correction was based on laboratory work in which an accounting was made for the water that is actually absorbed by the aggregate during the CorGsb determination. Thus the assumption of insignificant water ingress during CorGsb determination, as discussed earlier, has been partially dealt with in the AggSpec software.

In the specially prepared spreadsheet currently used by MoDOT, Instrotek applied corrections to both CorGsb and CorGsa values for fine and coarse aggregates. The CorGsa correction is a simple linear correlation equation that directly predicts T 84/85 Gsa. However, the CorGsb correction still poses a problem in that it is arrived at through a series of calculations that begin with the use of three simple linear predictive models utilizing T 84/85 ABS as the response (dependent) variable and CorABS (i.e. that absorption calculated using CorGsa and CorGsb values; see Equation 5 below) as the predictor (independent) variable.

$$\text{CorABS} = \frac{1 - \left(\frac{\text{CorGsb}}{\text{CorGsa}} \right)}{\text{CorGsb}} \times 100\% \quad (5)$$

The three ABS predictive models were developed using some of the MoDOT data utilized in this study and each covers a portion of the total range of absorption. One model covers CorABS values from 0 to 0.8%, a second covers 0.9 to 2.7%, and the third covers CorABS values greater than 2.8%. The models not only have gaps between them (0.8 to 0.9%, and 2.7 to 2.8%), but the predicted ABS values change drastically across these gaps.

Once a predicted ABS value is obtained, a calculated SSD weight for that sample is determined. Next, this SSD weight is combined with a calculated submerged sample weight based on a corrected CorGsa, and corrected bulk specific gravity is finally calculated. The circuitous nature of this process seems tedious at the best.

This correction method is doubly problematic in that absorption is the most imprecise measurement of the properties Gsa, Gsb, and ABS, as documented in the single-operator precision statements in T 84/85 and American Society for Testing and Materials (ASTM) C 128, "Standard Test Method for Density, Relative Density (Specific Gravity), and Absorption of Fine Aggregate."

The questionable methodology of using a series of discontinuous models to predict ABS was essentially the genesis of this study. Initial thoughts were to somehow connect the three different predictive models and remove the gaps between them. However, it soon became clear that the entire CoreLok calibration procedure needed to be re-examined. Similar to the simple correlation of CorGsa to Gsa as utilized in the current CoreLok worksheet designed for MoDOT, a more direct prediction of Gsb was desired. As a consequence of improved predictions of the two specific gravities, it was assumed that predicted ABS values would also be improved relative to the results of the procedure outlined above.

Objective

The objective of this work is to improve on the current calibration methods by developing models through regression analyses that will more reliably predict T 84/85 specific gravity and absorption values based on results from the CoreLok method. Increased confidence in using the CoreLok method for determining these properties could be useful to MoDOT in Quality Control, Quality Assurance (QC/QA) programs and/or routine laboratory testing by 1) reducing the time traditionally spent running these tests and 2) decreasing the variability between operators in order to minimize conflicts.

INVESTIGATION

As there was no laboratory work performed specifically for this study, the tasks involved the compilation, organization, and analysis of existing data only.

Data Compilation/Organization

MoDOT began performing aggregate tests using the CoreLok method and Instrotek's AggSpec software around July, 2002. As described earlier, a specially designed spreadsheet was implemented in the recent past to supplant the AggSpec software. The majority of the data is based on tests performed on samples that were considered coarse or fine aggregate. Later, however, MoDOT began running tests on samples with a combined gradation; i.e. materials that included coarse as well as fine fractions.

Prior to the beginning of this study, all data that MoDOT possessed concerning the CoreLok method and the associated T84/85 data was supplied to the authors. The compilation of the data began by modifying most of the electronic spreadsheets in order to view not only the raw weight data and the reported (corrected) CoreLok bulk and apparent specific gravity and absorption values, but the initial or non-corrected CorGsb and CorGsa calculated values as well because it was CorGsb and CorGsa that were to be used in the regression analyses.

Once the data was configured for complete accessibility, verification of the data that was included in summary worksheets was initiated. These summary worksheets were generated recently by MoDOT using the special spreadsheet format. This process of verification took a considerable amount of time as the summary sheets included not only data from the earlier AggSpec software but test results that had been obtained recently. Many of the CoreLok results reported in the summary sheets had to be replaced with the non-corrected Gsb and Gsa values.

Having devised a method for obtaining and verifying data to be used in the analysis, organization of said data was the next step. Of major importance in this process was the retention of the MoDOT sample identification (ID) label. The sample ID was used to sort through the data to discover redundancies and replication. If redundant data existed (all results being identical), all but one entry was removed. If replication existed (same sample ID and AASHTO results, different CoreLok test results), the results were averaged and used in the analysis. Exceptions to this rule were two high specific gravity samples (porphyry and steel slag). A special set of averaged replicated data (11 different samples in total) that resulted from a Round Robin study sponsored by MoDOT during late 2005 was also included in the overall dataset.

MoDOT had also color-coded the sample ID in order to identify whether the material was a fine or coarse aggregate. Additionally, color was used to identify samples with which there were associated fine and coarse test results; i.e. a combined gradation material split on the #4 sieve and the fine and coarse fractions tested separately. The accurate labeling of the sample as a fine, coarse, or combined gradation aggregate was also verified using the raw weight data in the CoreLok spreadsheets. The following is a list of the column heading labels in the basic spreadsheet created for data analysis and an explanation of its meaning:

- SAMPLE ID
- FINES (Each sample was coded as either 0 or 1; 0 meaning no -#4 material in the sample and 1 meaning -#4 material is in the sample)

- CORTEST (Each sample was coded as either 0 or 1; 0 meaning the CoreLok test was performed in the large pycnometer and 1 if it was performed in the small pycnometer. This coding in conjunction with the FINES label helped identify whether the sample was a combined gradation)
- AASHTO (Each sample was assigned the label T 84, T 85, or AVG depending on which AASHTO test method was used to determine the associated Gsb, Gsa, and ABS values. AVG indicated that the sample was a combined gradation and a weighted average of T 84 and T 85 results was calculated and reported)
- GSB (AASHTO bulk specific gravity, oven-dry basis)
- GSA (AASHTO apparent specific gravity)
- ABS (AASHTO absorption)
- CORGSB (Non-corrected CoreLok bulk specific gravity, oven-dry basis)
- CORGSA (Non-corrected CoreLok apparent specific gravity)
- CORABS (This value was calculated using CorGsb and CorGsa)

The initial compilation of data resulted in a total of 233 unique samples (spreadsheet rows) that were either a fine, coarse, or combined gradation aggregate. The aggregate types included mostly crushed carbonate stone (limestone, dolomite, or dolomitic limestone), some natural sands/gravels and flint chats, a few granite, quartzite, and porphyry samples, and 6 different steel and power plant slag samples. As a check on the mathematical validity of the 233 individual datasets, the difference between the apparent and the bulk specific gravity (both AASHTO and CoreLok) was calculated to make sure there were no negative differences because apparent should always be larger than bulk specific gravity.

Overall Dataset Modification

Having compiled the overall dataset, a modification was performed in response to a concern expressed by MoDOT regarding T 84 test results. As discussed earlier, the issue centers on the reliability of T 84 test results except in the case of natural sands or flint chats; i.e. fine aggregates with relatively smooth surfaces, rounded shapes, and few fines. MoDOT felt that unless the aggregate was a natural sand or flint chat, it should be removed from the analysis. However, if the aggregate was something other than natural sand or flint chat but there was an associated T 85 test result for that same material, the fine aggregate test results should remain in the analysis with the associated T 85 specific gravity and absorption values being assigned to that fine aggregate. MoDOT argued further on a theoretical basis that because most of the fine aggregate in question resulted from the crushing/processing of quarried carbonate stone originating from relatively uniform geologic formations/ledges (e.g. manufactured sands), the fundamental properties of specific gravity and absorption should remain relatively constant despite particle size. Therefore after making the modifications requested, the result was a total of 200 individual datasets to be used for analysis purposes.

In order to provide for an independent set of data to be used for model validation purposes, the 200 sample dataset was reduced to 180 for model development with the remaining 20 samples set aside for model validation. The process began with the temporary removal of the few high specific gravity aggregates MoDOT considered essential to keep in the larger dataset to be used for model development: 2 porphyry ($G_{sa} > 2.9$) and 5 steel slag samples ($G_{sa} > 3.5$). The remaining 193 sample datasets were assigned a randomly generated integer between 1 and 193. These random numbers were then sorted in an ascending order thereby shuffling the sample datasets in a random fashion. Finally, the first and last 10 rows were selected to be used as the model validation dataset, and the remaining 173 were recombined with the 7 high specific gravity samples to produce the 180 sample dataset used for regression analysis purposes (included in the appendix).

Statistical Analysis Methodology

The predictive model development procedure was implemented through the use of several different software packages designed for statistical analysis and/or curve-fitting procedures: SAS, Minitab, SigmaStat, JMP IN, TableCurve 2D, and TableCurve 3D. Each program allows for the direct importation of Excel spreadsheets. SAS was used mainly for collinearity diagnostics; verifying through quantification whether the predictor variables (e.g. CorGsb, CorGsa, etc.) are sufficiently independent of each other so that any model using those predictor variables is stable. Minitab was used to perform paired T-tests (determining whether two groups are statistically different), linear least squares regressions, and to produce correlation matrices. SigmaStat was used to perform non-linear least squares regressions. JMP IN is an educational package produced by SAS that is relatively easy to use and can perform stepwise model selection procedures as well as standard least squares regressions with predictor variable interactions. TableCurve 2D (one predictor variable) and 3D (two predictor variables) are curve-fitting programs that are extremely useful when the analysis involves a small number of predictor variables. One can automatically fit 3667 built-in equations using TableCurve 2D and approximately 37,000 built-in equations with TableCurve 3D. At some point in the analysis, each one of these programs was used, some more than others.

The first step in the regression analyses was to determine potential predictor variables for each response variable of interest using theoretical considerations and/or correlation matrices. The primary example of theoretical considerations guiding the model development process focused on the CorGsb determination process. It was assumed from the beginning that aggregate absorptive properties were influencing the CorGsb results as discussed earlier. Therefore, a Gsb predictive model was envisioned as potentially having the following form:

$$\text{Gsb} = \text{CorGsb} + \text{difference} + \text{error} = \text{CorGsb} + f(\text{absorptive property}) + \text{error} \quad (6)$$

The absorptive property that probably has the greatest effect on the amount of water absorbed by the aggregate during the two minute time period is rate of absorption. However, the authors are not aware of any generally accepted measurement method, quantitative or qualitative, for this particular property. Therefore, the only measurement that has some correlation with rate of absorption is absorption as defined in Equation 4. As indicated earlier, absorption is defined as the weight of water taken into the water-permeable voids of the aggregate over a specified length of time, under static submersion, at atmospheric pressure and room temperature, and expressed as a percentage of the mass of the solids. Thus absorption is a function of both rate of absorption (how fast water moves through the voids) and absorptive capacity (amount of water the voids can ultimately hold). Therefore, it was intuitive to investigate ABS and CorABS as potential predictor variables for Gsb.

The correlation matrix is one of the quickest methods for determining if there is any linear relationship between two variables. Reported values in the correlation matrices utilized in this study were the Pearson correlation coefficient (essentially the square root of R^2) and the p-value of the correlation. For example, a high correlation coefficient (e.g. > 0.5) and a low p-value (e.g. $\leq \alpha = 0.05$) indicates a strong and significant degree of collinearity.

Having gained a good idea of which predictor variable(s) to use per response variable, several different model types were investigated in the regression analyses. Some of the models used were simple linear (one predictor), multiple linear (two or more predictors), multiple linear with interactions (products of two or more predictors), non-linear power law, and a host of complex models imbedded in the TableCurve software packages. The two primary response variables were Gsa and Gsb. Although a predictive model for ABS was investigated, the intention from the

beginning was to obtain Gsa and Gsb predicted values and then calculate ABS using the same formula as shown in Equation 5.

A list of the best models for each response variable was compiled with the primary criteria for inclusion in the list being a high predicted R^2 value (R^2_{pred}). R^2_{pred} is the preferred parameter for determining how well the model will predict new observations whereas R^2 (and adjusted R^2) only indicates how well the model fits the data. This goodness-of-fit statistic was not the only criteria for model selection, however. The predictor variables had to be significant at an $\alpha = 0.05$ level and they needed to be sufficiently independent of one another (excluding interactions). Significance level was determined using the aforementioned p-value. Variable inter-dependence, usually called multi-collinearity, was measured using variance inflation factors (VIF), and proportion of variance values in conjunction with condition indices.

Next, all possible combinations of the best models for predicting Gsa (Gsa_{pred}) and Gsb (Gsb_{pred}) based on the criteria outlined above were used to calculate a predicted ABS value (ABS_{pred}). After a thorough check to make sure no negative absorption values were generated, the numerous sets of ABS_{pred} values were then compared against T 84/85 ABS values using paired T-tests and simple linear regressions. This comparison process was the final step in determining the recommended Gsa_{pred} and Gsb_{pred} models.

Therefore in summary, the specific gravity predictive models that best satisfied both of the following sets of criteria were recommended:

1. Sufficiency of the regression analysis statistics goodness-of-fit (R^2_{pred}), predictor variable significance (p-values), and predictor variable independence (VIF and proportion of variance).
2. Best possible comparison of the calculated absorption values based on predicted specific gravity values with T 84/85 absorption values.

Secondary Analyses

In the early stages of discussion concerning this work, MoDOT had the view that whenever a new aggregate source was being evaluated for use, T 84/85 tests would still be performed to determine the reference or “true” specific gravity and absorption values, and the CoreLok method would be utilized primarily for QC/QA purposes. Additionally, it was thought that T 84/85 ABS would continue to be the primary parameter used in the CoreLok method bulk specific gravity calibration procedure in much the same way as described earlier, except that the three distinct and discontinuous absorption predictive models would be replaced with one continuous model. But what if ABS is not available?

In an attempt to answer this question, the calculated CorABS value (Equation 5) was investigated as a substitute for ABS as indicated earlier. This particular analysis was performed concurrently with the main analysis using the 180 sample dataset.

As an alternative method to answering the question posed above, an analysis was undertaken in which Micro-Deval and Los Angeles Abrasion (LAA) values were investigated as potential predictor variables. Both tests are aggregate quality indicators and are a function of the geology of the material. The Micro-Deval test is a durability test that measures resistance to abrasion in the presence of water while the LAA test is a durability test that measures resistance to abrasion and impact in a dry condition. Micro-Deval and LAA test data for the aggregates included in the overall dataset was compiled resulting in 161 LAA and 169 Micro-Deval individual datasets for analysis purposes. Some of the same statistical analysis procedures outlined above were applied to this particular dataset. It should be noted, however, that the sources for the Micro-Deval and LAA data were varied, and the associations of the particular test results to the dataset samples were not always clear.

RESULTS AND DISCUSSION

Although there were many acceptable calibration or predictive models generated, only the recommended models are presented here.

Variable Correlations and Comparative Analyses

Unless otherwise specified, all results presented in the following sections are based on the 180 sample dataset. Table 1 gives the correlation matrix for the relevant variables.

Table 1: Correlation Matrix

| Variable | Statistic | Fines | Gsb | Gsa | ABS | CorGsb | CorGsa |
|----------|-----------|---------------|---------------|--------------|--------------|--------------|--------------|
| Gsb | Pearson* | -0.001 | | | | | |
| | p-value | 0.984 | | | | | |
| Gsa | Pearson* | -0.099 | 0.921 | | | | |
| | p-value | 0.187 | 0.000 | | | | |
| ABS | Pearson* | -0.249 | -0.363 | 0.022 | | | |
| | p-value | 0.001 | 0.000 | 0.771 | | | |
| CorGsb | Pearson* | -0.087 | 0.938 | 0.973 | -0.082 | | |
| | p-value | 0.246 | 0.000 | 0.000 | 0.271 | | |
| CorGsa | Pearson* | -0.110 | 0.896 | 0.982 | 0.043 | 0.983 | |
| | p-value | 0.142 | 0.000 | 0.000 | 0.565 | 0.000 | |
| CorABS | Pearson* | -0.165 | -0.060 | 0.225 | 0.679 | 0.089 | 0.267 |
| | p-value | 0.027 | 0.420 | 0.002 | 0.000 | 0.236 | 0.000 |

* Pearson product moment correlation coefficient

The Pearson correlation coefficient ranges from -1 to +1 and measures the degree of linear relationship between the two variables. The sign on the coefficient indicates the direction of the correlation; e.g. if the sign is negative, one variable increases as the other decreases. The magnitude of the coefficient indicates the strength of the correlation.

The p-value indicates the significance of the correlation; the smaller the p-value, the greater the significance of the correlation. In most instances, an $\alpha = 0.05$ significance level is chosen as the threshold value to compare p-values against when making inferences or drawing conclusions. Such is the case throughout this analysis. Those correlations that are considered significant have been highlighted through the bolding of the p-value and correlation coefficient. One must consider, however, that some of the significant correlations are partially the result of mathematical constructs. For example, CorGsa and CorGsb are used to calculate CorAbs. Therefore, it would be logical that some correlation would exist between these variables.

Of special interest is the correlation between Fines and ABS/CorAbs, remembering that the variable Fines is coded as 0 if the sample is all +#4 material and 1 if some -#4 material is present. Therefore based on the sign of the correlation coefficient, absorption decreases as the fine content increases. This observation supports one of the theoretical arguments made by a MoDOT materials engineer. According to the theory, the probability is higher that failure surfaces created during the process of

crushing aggregate will pass through the voids, permeable and non-permeable. These voids are, therefore, transformed into particle surface features that are no longer considered part of the aggregate particle bulk volume. Therefore, the percentage of water-permeable voids volume per unit bulk volume of aggregate is decreased as particle size is decreased. Thus, absorptive capacity on a unit bulk volume basis is also decreased.

More to the point of this work are the correlations between Gsb and Gsa to CorGsb and CorGsa, respectively. The correlation coefficient values show that the Gsa/CorGsa correlation is stronger than the Gsb/CorGsb correlation. Additionally, the ABS/CorABS correlation is significant, but substantially weaker than the Gsb and Gsa correlations with their counterparts. This ranking of correlations agrees with the single-operator precision statements in T 84/85 and American Society for Testing and Materials (ASTM) C 128, “Standard Test Method for Density, Relative Density (Specific Gravity), and Absorption of Fine Aggregate.” Paired T-test results of the T 84/85 and associated CoreLok results are given in Table 2.

It should be noted that one of the primary assumptions in statistical analyses is that the data fits some distribution, which with many types of test data is usually a normal distribution. However, a series of Anderson-Darling normality tests on the 180 sample dataset shows that none of the test results are normally distributed. The differences, although still not normally distributed, do have better (lower) Anderson-Darling statistics indicating more normality than the actual test results with absorption differences being the most normal. Therefore conclusions presented about the statistical analyses, although not invalid, should be considered in the light of this lack of normality.

Table 2: Paired T-Test Results

| Parameter | N | Mean | St Dev | T-value | p-value | Lower | Upper |
|----------------------------|-----|---------|--------|---------|---------|---------|---------|
| Gsb | 180 | 2.633 | 0.161 | | | | |
| CorGsb | 180 | 2.716 | 0.168 | | | | |
| Difference* | 180 | -0.0833 | 0.0583 | | | | |
| T-Test of Mean Difference | | | | -19.16 | 0.000 | | |
| 95% CI for Mean Difference | | | | | | -0.0919 | -0.0747 |
| Gsa | 180 | 2.755 | 0.164 | | | | |
| CorGsa | 180 | 2.772 | 0.186 | | | | |
| Difference* | 180 | -0.0171 | 0.0398 | | | | |
| T-Test of Mean Difference | | | | -5.76 | 0.000 | | |
| 95% CI for Mean Difference | | | | | | -0.0229 | -0.0112 |
| ABS (%) | 180 | 1.668 | 0.890 | | | | |
| CorABS (%) | 180 | 0.727 | 0.443 | | | | |
| Difference* (%) | 180 | 0.941 | 0.672 | | | | |
| T-Test of Mean Difference | | | | 18.77 | 0.000 | | |
| 95% CI for Mean Difference | | | | | | 0.842 | 1.0399 |

* Difference = (T 84/85 value) – (CoreLok value)

There is a lot of information in Table 2 concerning the relationships between T 84/85 and CoreLok test results. For example, the CoreLok method returns higher bulk and apparent specific gravity results, on average, than the standard T 84/85 methods. Also, the mean difference between Gsa and CorGsa is smaller than the mean difference between Gsb and CorGsb which supports the Table 1 results showing a stronger correlation between Gsa and CorGsa than between Gsb and CorGsb. The T-value or T-test statistic is a measure of the distance of the mean difference from zero and is used to calculate the p-values. Using a significance level of $\alpha = 0.05$, the p-values for all three comparisons show that the differences are highly significant; i.e. for the differences to approach zero, some calibration is necessary. Finally, the lower and upper bounds of the 95% confidence interval (CI) for the mean differences do not encompass zero and show in a different way that the differences are statistically significant. Figures 1, 2 and 3 show the histogram of differences of these three properties.

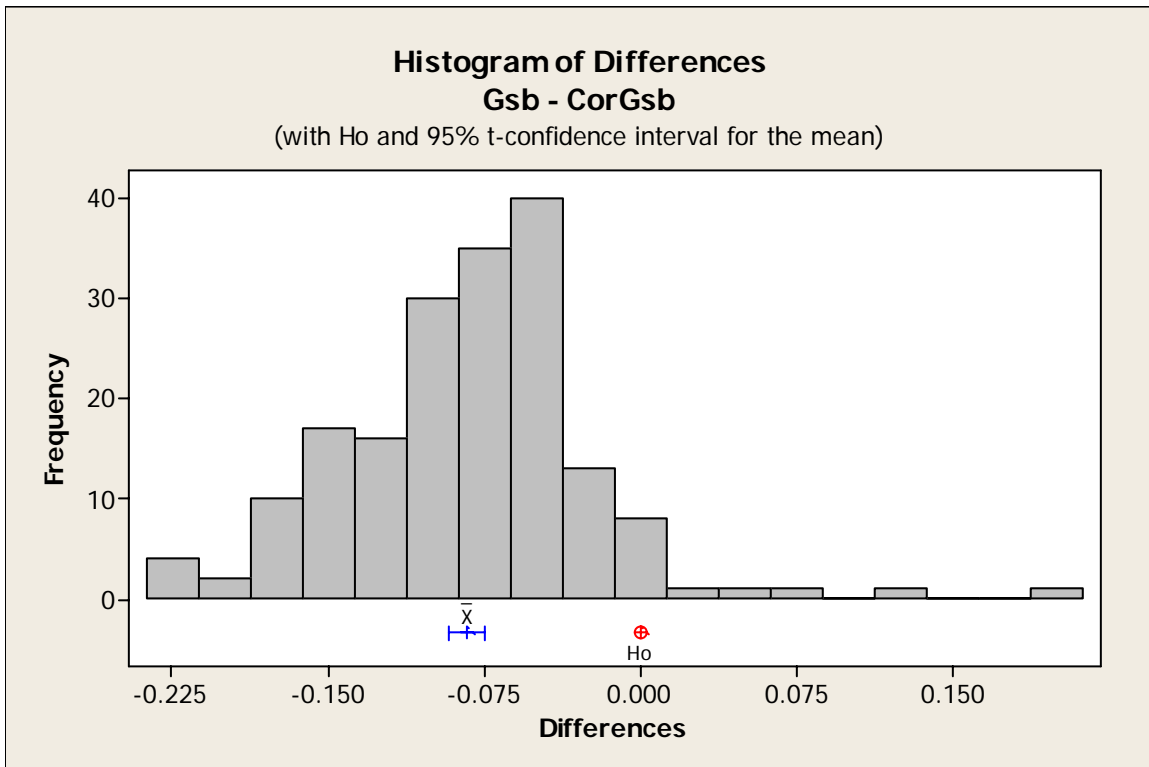


Figure 1: Histogram of Differences: Gsb – CorGsb

A brief explanation of these figures may be helpful. The histogram shows the general shape of the distribution of the differences. The symbol labeled as Ho is defined as the null hypothesis; i.e. the mean difference between Gsb and CorGsb = 0. The null hypothesis is analogous to the assumption in the U.S. justice system that one is innocent until proven guilty. In our situation, the alternative hypothesis is that the mean difference between Gsb and CorGsb $\neq 0$, or in the legal analogy, the evidence is such that one has been proven guilty, beyond a reasonable doubt. One could say that the significance level, α , is the threshold that a reasonable person would say has to be crossed before the evidence is convincing. The symbol \bar{X} is the mean difference with the associated 95% CI right below it. If the CI does not overlap Ho, then we reject the null hypothesis; i.e. the evidence is sufficient to accept the alternative hypothesis that there is a difference between Gsb and CorGsb.

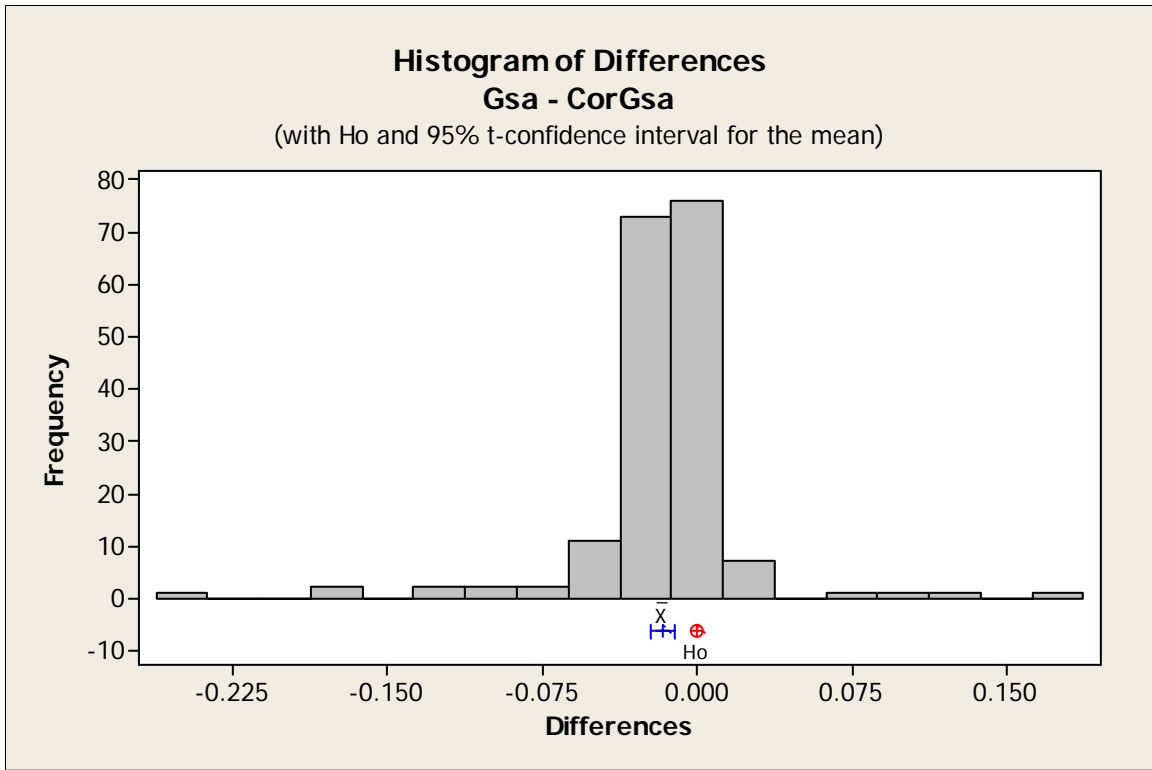


Figure 2: Histogram of Differences: Gsa – CorGsa

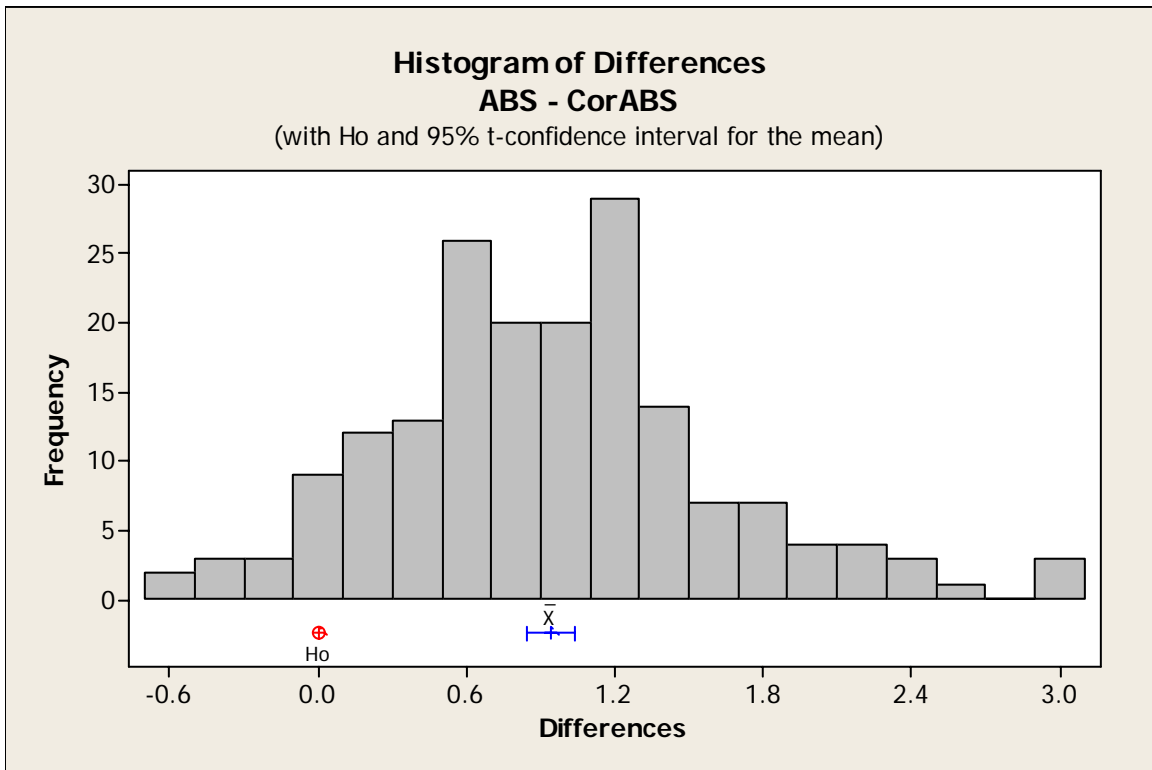


Figure 3: Histogram of Differences: ABS – CorABS

Figure 2 really shows the lack of variability about the mean difference when determining apparent specific gravity relative to the bulk specific gravity differences depicted in Figure 1. Based on the analyses in this section, one would expect that any correction to be made to the CorGsa determinations in order to predict Gsa values would be minimal compared to the CorGsb correction.

Predictive Models

Apparent Specific Gravity: Gsa

The various regression analyses resulted in a total of 9 different Gsa predictive models that met all the criteria outlined earlier. Interestingly but not surprisingly, the R^2_{pred} values had a very narrow range; 0.9627 to 0.9655. With CorGsa as the only predictor variable, a simple linear regression using the least squares method resulted in an $R^2_{\text{pred}} = 0.9627$. As indicated in Table 1, the correlation of Gsa to ABS was insignificant. But ABS did show up occasionally in the model selection process as being statistically significant when used as an additional predictor variable in the regression analyses. CorABS, on the other hand, did have a strong and significant correlation to Gsa as shown in Table 1, and was a more powerful co-predictor than ABS. Therefore, the recommended model for predicting Gsa has CorGsa and CorABS as the predictor variables and is given below:

$$Gsa_{\text{pred}} = 0.24680896 + 0.90993947(\text{CorGsa}) - 0.02031058(\text{CorABS}) \quad (7)$$

| | |
|------------------------------|---------|
| Where: $R^2_{\text{pred}} =$ | 0.9641 |
| Intercept p-value = | 0.00000 |
| CorGsa p-value = | 0.00000 |
| CorABS p-value = | 0.00024 |
| VIF of CorGsa = | 1.07668 |
| VIF of CorABS = | 1.07668 |

The statistics associated with Equation 7 show a high degree of predictive power and highly significant predictor variables (p-values $\lll \alpha = 0.05$). The fact that the R^2_{pred} for Equation 7 is not the highest of the range indicated in the previous paragraph goes to the recommendation criteria summarized earlier: 1) sufficient predictive characteristics and 2) optimum comparison of the calculated absorption to the T 84/85 ABS values. The model that produced the highest R^2_{pred} value did not necessarily produce the best predicted absorption values. The variance inflation factors (VIF) indicate slight correlation between CorGsa and CorABS which was expected. However based on generally accepted criteria, there is not enough correlation to cause problems with the regression coefficients. Minitab, for example, states that if $VIF = 1$, there is no relation between the variables. If the VIF is between 1 and 5, there is some correlation and it increases with increasing VIF. If $VIF > 5$, the correlation is severe and the regression coefficients may be in question. The VIF values shown in Equation 7 were actually determined using the original 200 sample dataset.

Equation 7 was generated using TableCurve 3D. The model is of a linear form however the regression procedure was not the standard least squares method. Equation 7 was the result of a “robust” regression procedure within TableCurve 3D. The purpose of robust regression is to reduce the influence of outlying observations. Instead of making “judgments” about individual observations in a dataset as to whether they should be removed or should remain, a robust regression uses all the data and accounts for high variance in these questionable observations using statistical methods. The inclusion of the high specific gravity porphyry and steel slag in the dataset dictated that robust regression should be investigated as an alternative to standard least squares.

Also note that although the inclusion of CorABS as a predictor variable for G_{sa_pred} does not substantially increase the R^2_{pred} relative to the simple linear model described above ($R^2_{pred} = 0.9627$), its ultimate usage was the result of the accuracy with which absorption could be later calculated (relative to T 84/85 ABS) using G_{sa_pred} and G_{sb_pred} . Figure 4 shows the plot of the predicted G_{sa} values versus the measured T 84/85 values.

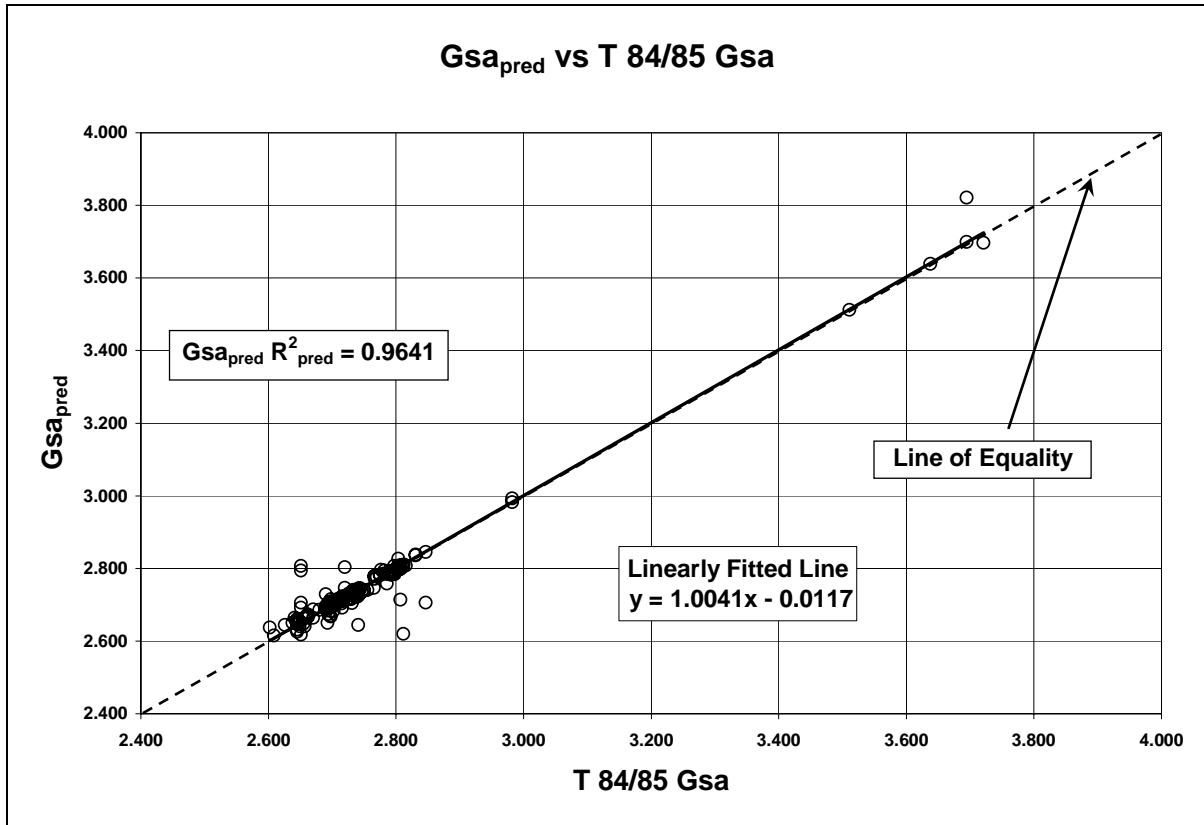


Figure 4: Predicted vs. Measured T 84/85 Apparent Specific Gravity

The linearly fitted line equation shown in Figure 4 indicates the quality of Equation 7. The slope of the line is very near 1.0000. It is positioned almost exactly on top of the line of equality meaning that the two methods of producing G_{sa} values are equivalent with no bias toward over or under-prediction, based on the 180 sample dataset.

Bulk Specific Gravity: Gsb

A total of 10 different G_{sb} predictive models were developed. Again, all criteria outlined earlier were met in these models. R^2_{pred} values ranged from 0.8764 to 0.9624. Unlike the G_{sa} analysis, ABS is more powerful than CorABS in predicting G_{sb} . This means that T 84/85 tests will have to be run prior to using the recommended G_{sb} predictive model. However as discussed earlier, the performance of T 84/85 is MoDOT's default process when evaluating a new aggregate source. The recommended model (shown below) can therefore be used as part of a QC/QA plan or as an interim laboratory procedure to track changes. An alternative model that uses CorABS as a substitute for ABS will be presented in a later section.

$$Gsb_{pred} = 0.342355 + 0.8751137(CorGsb) - 0.051843(ABS) \quad (8)$$

Where: $R^2_{pred} = 0.9598$
 Intercept p-value = <0.0001
 CorGsb p-value = <0.0001
 ABS p-value = <0.0001
 VIF of CorGsb = 1.006841
 VIF of ABS = 1.006841

Except for the R^2_{pred} being slightly lower than that for Equation 7, the other relevant statistics for Equation 8 are almost ideal; very high significance and very low multi-collinearity within the predictor variables. Equation 8, as it turns out, is the simplest two-factor Gsb model of all those developed and the standard least squares method was used in the regression procedure. The robust regression procedure was investigated for Gsb_{pred} , and the resultant model was ranked as number 2 out of the 10 models developed. However, Equation 8 was slightly superior to the robust model in best meeting the two general criteria for recommendation: 1) good regression statistics and 2) optimum correlation between calculated and T 84/85 absorptions. Figure 5 shows the plot of the predicted Gsb values versus the measured T 84/85 values.

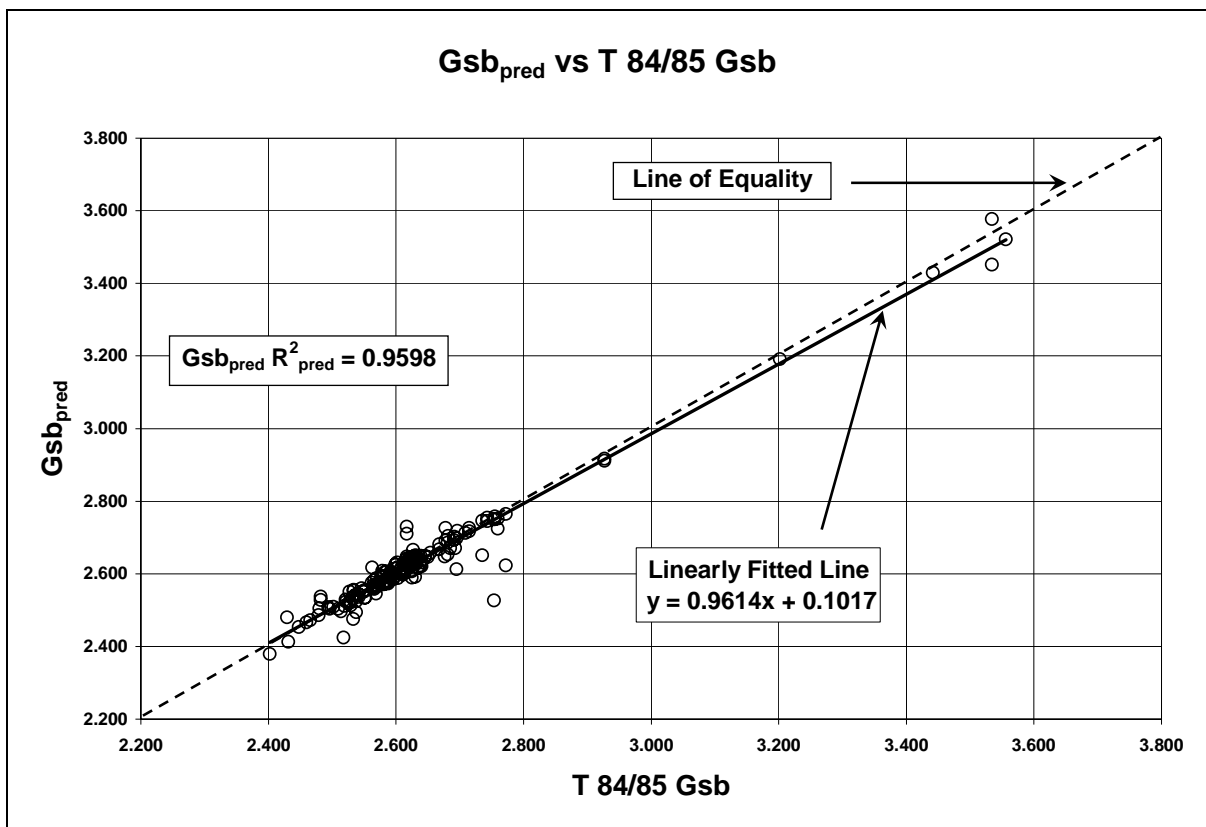


Figure 5: Predicted vs. Measured T 84/85 Bulk Specific Gravity

One notices right away in Figure 5 that there is a slight bias toward under-predicting Gsb as the values increase. This may be a consequence of using a very small number of high specific gravity aggregates in the analyses. These few data points had what is termed as high “leverage” in the

regression analysis that generated Equation 8. They overly influence the regression coefficients on the predictor variables so it is extremely important that, in this case, the CorGsb and ABS values for these high specific gravity samples were accurate.

Absorption: ABS

Calculating absorption by substituting the results of Equations 7 and 8 into Equation 5, and then comparing those calculated values to T 84/85 ABS values was used as the second general criteria for selecting the recommended $G_{sa_{pred}}$ and $G_{sb_{pred}}$ models. Initial attempts were focused on developing a predictive model for ABS based on CorABS and Fines. The results presented in Table 1 showing the significant correlation of Fines to ABS and CorABS gave indications that this strategy might be the preferred method. However, the best model based on this method resulted in a low $R^2_{pred} = 0.4997$. The model otherwise had very good significance and multi-collinearity statistics. The calculated ABS_{pred} based on $G_{sa_{pred}}$ and $G_{sb_{pred}}$ was far superior in its predictive power ($R^2_{pred} = 0.9412$) and is the recommended method for determining absorption based on the CoreLok method. Figures 6 and 7 show the histogram of differences and the predicted versus measured T 84/85 absorption values, respectively.

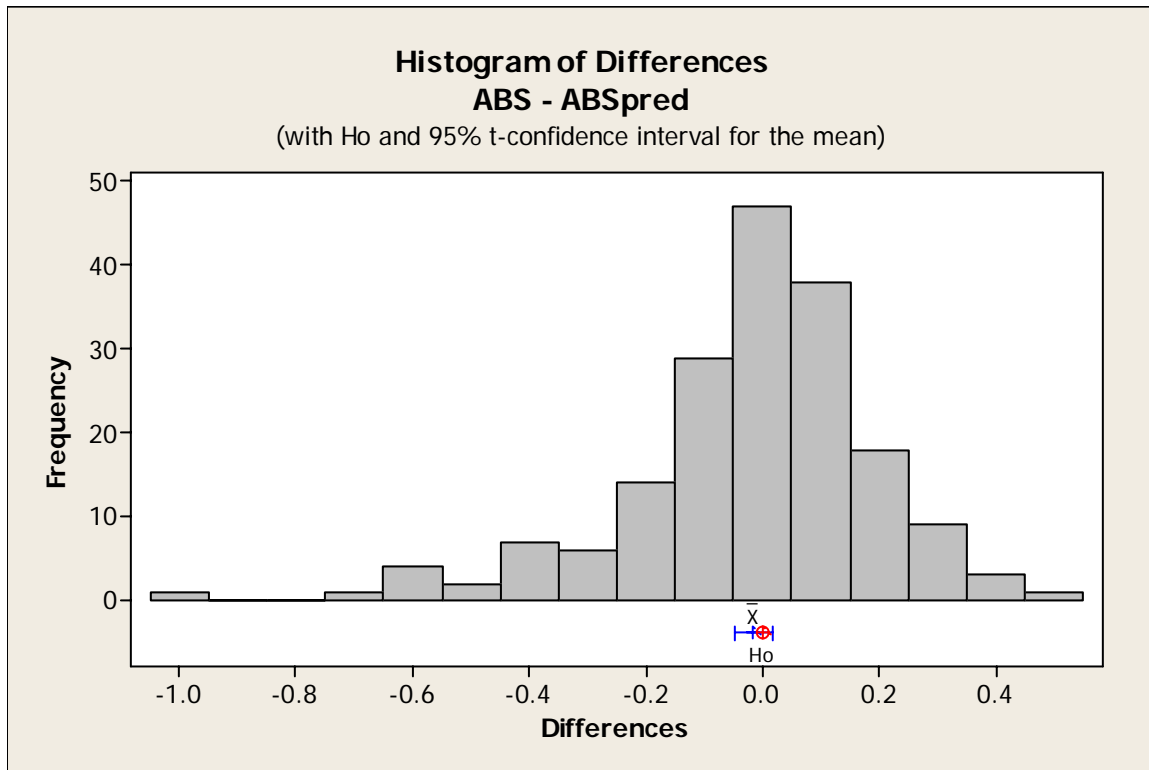


Figure 6: Histogram of Differences: ABS - ABS_{pred}

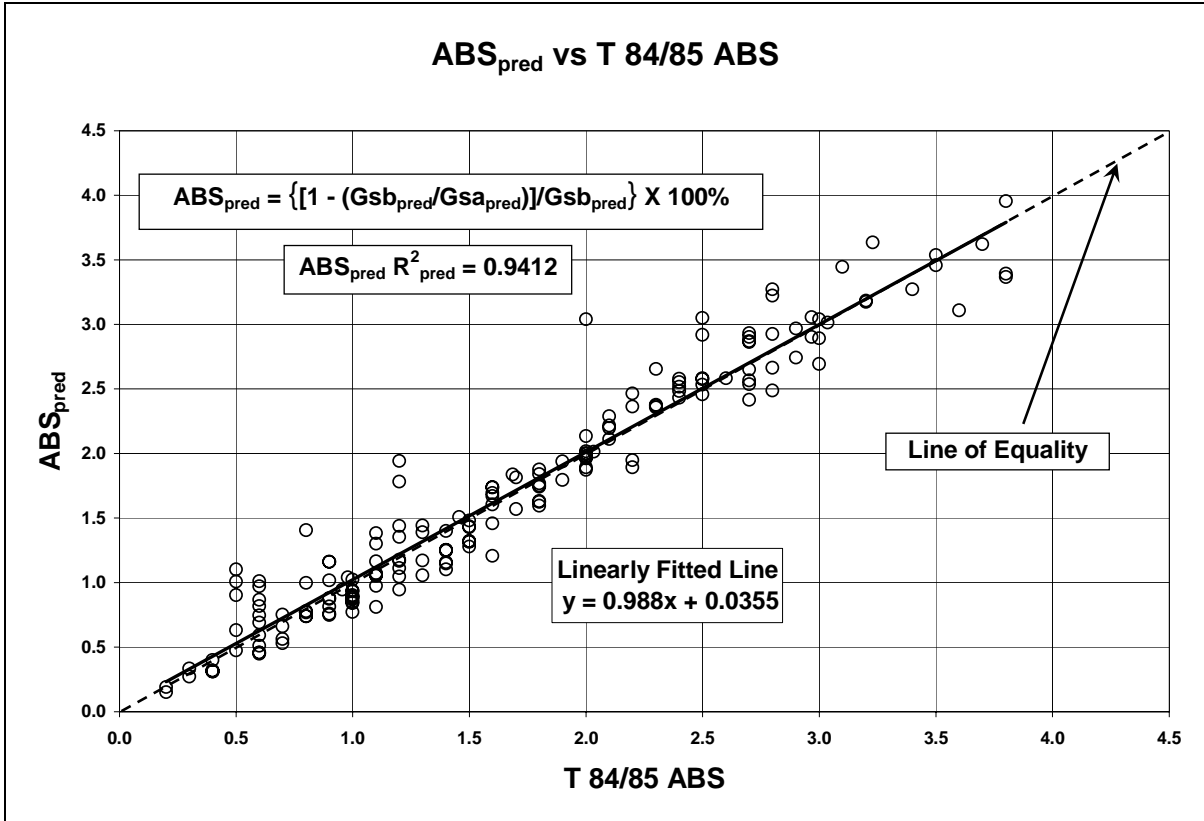


Figure 7: Predicted vs. Measured T 84/85 Absorption

Figure 6 indicates that there is statistically no difference between the two methods of determining absorption (at the 95% confidence level) and Figure 7 reinforces this conclusion as the linearly fitted line coincides almost exactly with the line of equality. Although not pursued in this work, one could follow this methodology and investigate the prediction of bulk specific gravity on the SSD basis using Gsb_{pred} and Gsa_{pred} in a mathematical calculation.

Alternate Bulk Specific Gravity Prediction

In the event that ABS is not available, CorABS in conjunction with CorGsb can be used to predict Gsb. The recommended model for this scenario is given below:

$$Gsb_{pred-alt} = e^{-\left[0.5172953 + 0.42536397(\ln(\text{CorGsb}))^2 + 0.047810382(e^{-\text{CorABS}})\right]} \quad (9)$$

Where: $R^2_{pred} = 0.9047$
 Intercept p-value = <0.0001
 CorGsb p-value = <0.0001
 CorABS p-value = <0.0001
 VIF of CorGsb = 1.00346
 VIF of CorABS = 1.00346

Equation 9 is a complex model with good statistics but a slightly lower level of predictive power relative to Equation 8. Simpler models were generated that utilized CorABS as a predictor variable,

but Equation 9 was the best overall in that it was superior when used as a factor in calculating a predicted absorption in conjunction with Equation 7 ($ABS_{pred-alt} R^2_{pred} = 0.5007$). Figure 8 shows the plot of predicted versus measured T 84/85 bulk specific gravity using Equation 9.

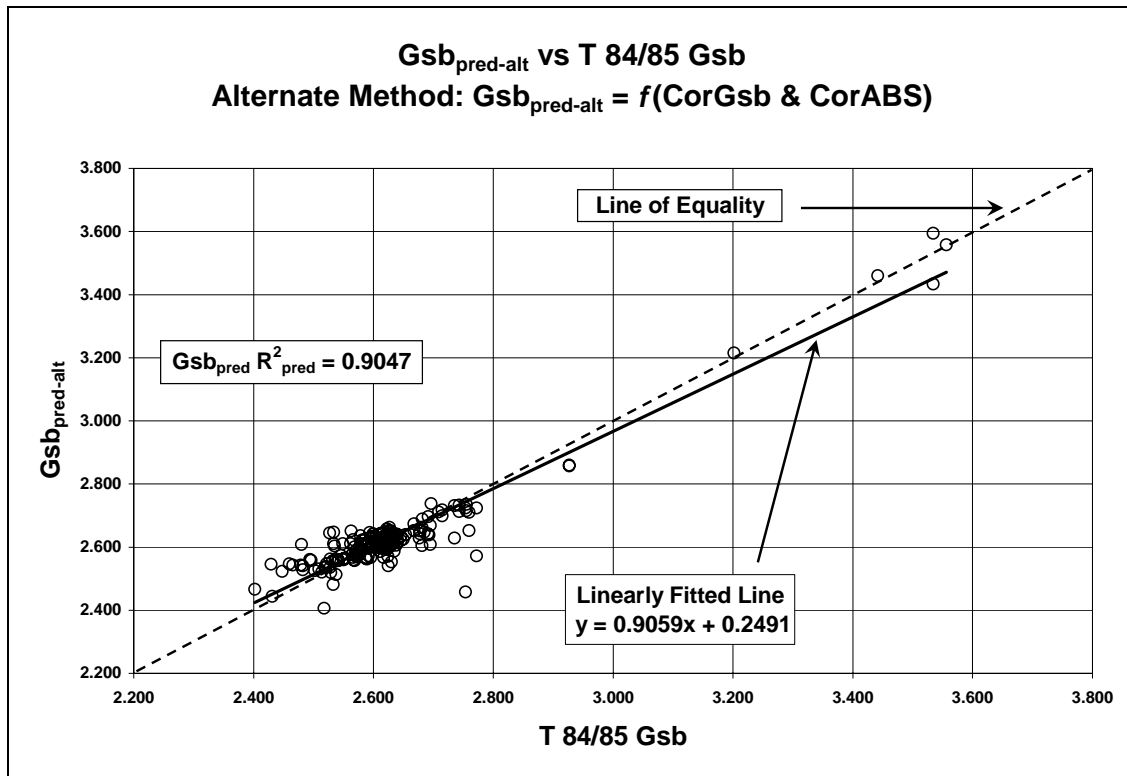


Figure 8: Predicted (Alternate) vs. Measured T 84/85 Bulk Specific Gravity

As with Equation 8, Equation 9 does exhibit some bias toward under-predicting at the higher values as shown in Figure 8. This particular type of bias is not overly problematic unless one is not aware of it or does not consider it when making inferences or conclusions about predictions.

Model Validation

As discussed earlier, 10% of the original 200 sample dataset was semi-randomly selected and set aside for model validation; semi-randomly because there was the prior removal of the 7 high specific gravity porphyry and steel slag samples prior to the randomization. The models given in Equations 7 and 8 were fit to these 20 samples that have been set aside and the plots of predicted versus measured T 84/85 values are presented below in Figures 9 through 11.

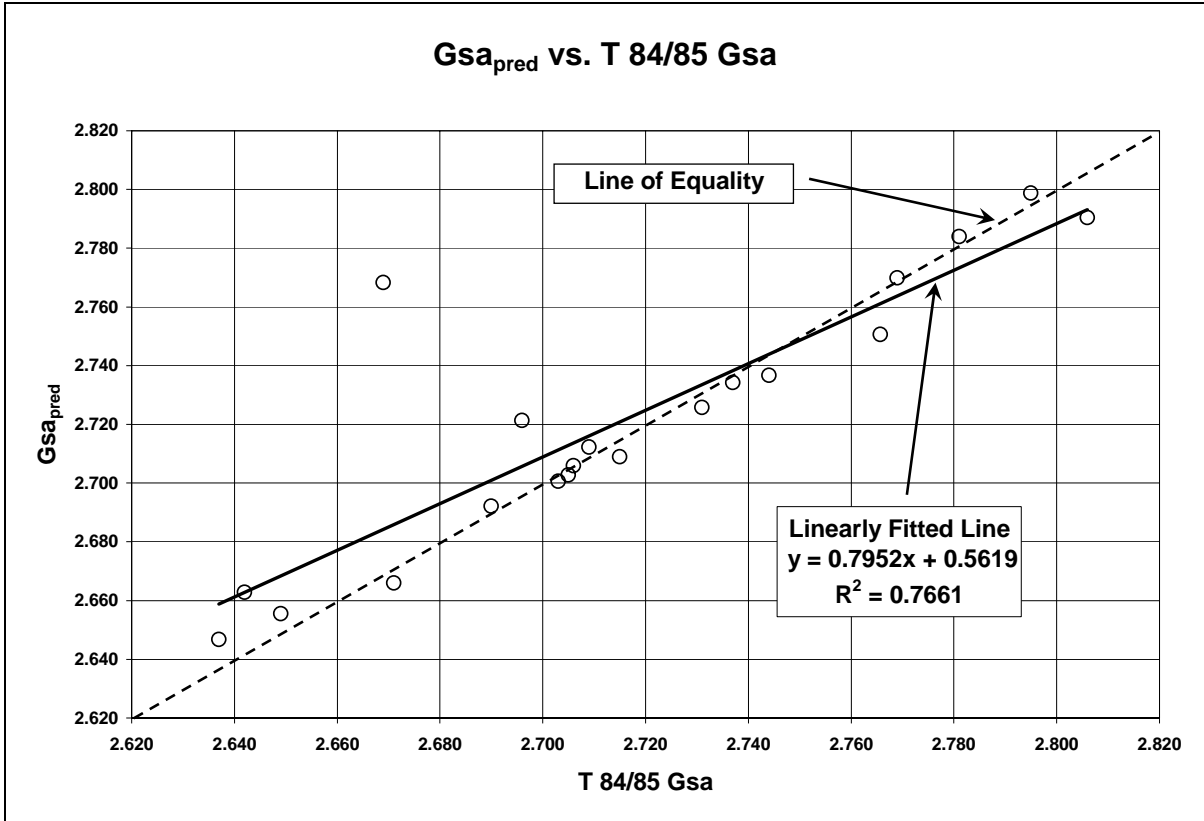


Figure 9: Model Validation: Gsa_{pred} vs. T 84/85 Gsa

Figure 9 shows considerable bias in the fit. There are some datapoints at each end of the T 84/85 Gsa data range that are exerting some leverage and there is one data point that could be considered an outlier, at least in this dataset. It is also important to remember that as the highest Gsa value in Figure 9 lies between 2.800 and 2.820, the predictive model was developed to cover a much higher upper range. Intuitively, one would think this is an advantage and it very well may be. However, it should not be assumed that a model characterizing a wide range of data will accurately describe localized behavior within portions of that overall range. For example, the steel slag is not a naturally occurring geologic material and there may be aspects of its properties that are inconsistent with how geologic materials behave or respond to physical or chemical inputs; i.e. there may be other factors that could be used to calibrate the steel slag CoreLok results to T 84/85 results other than those used in this analysis.

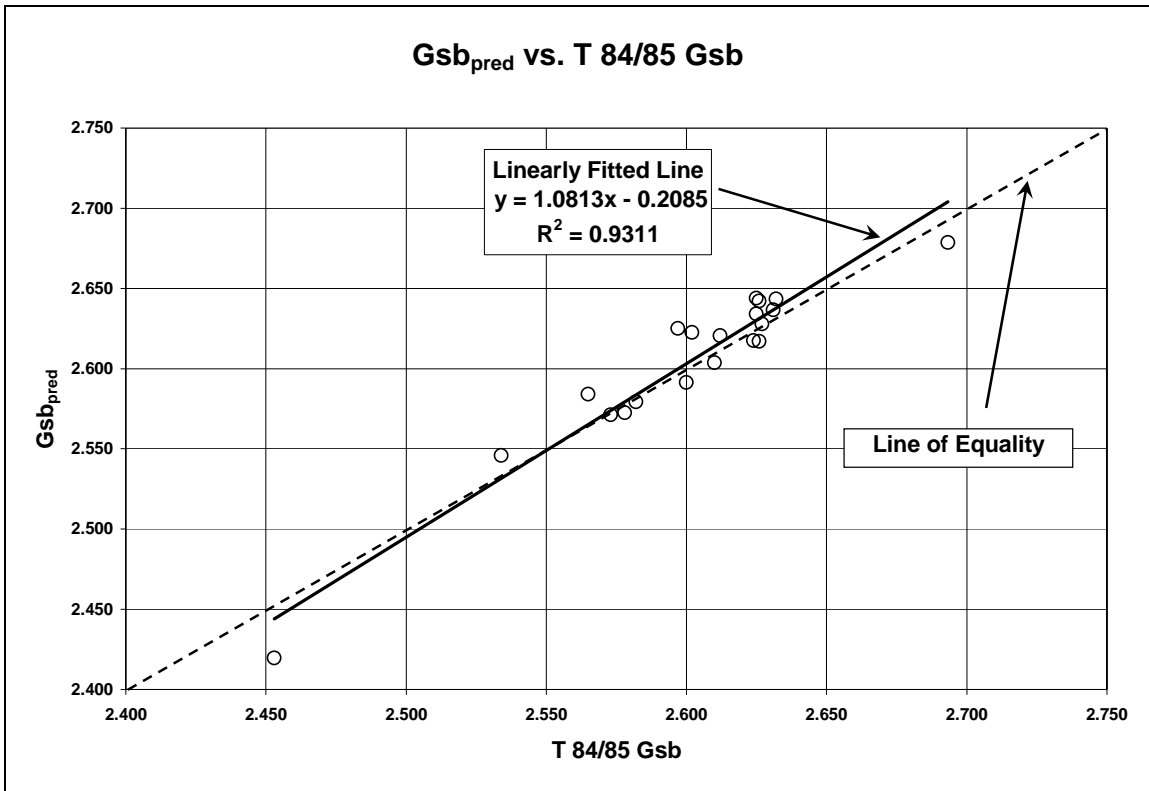


Figure 10: Model Validation: Gsb_{pred} vs. T 84/85 Gsb

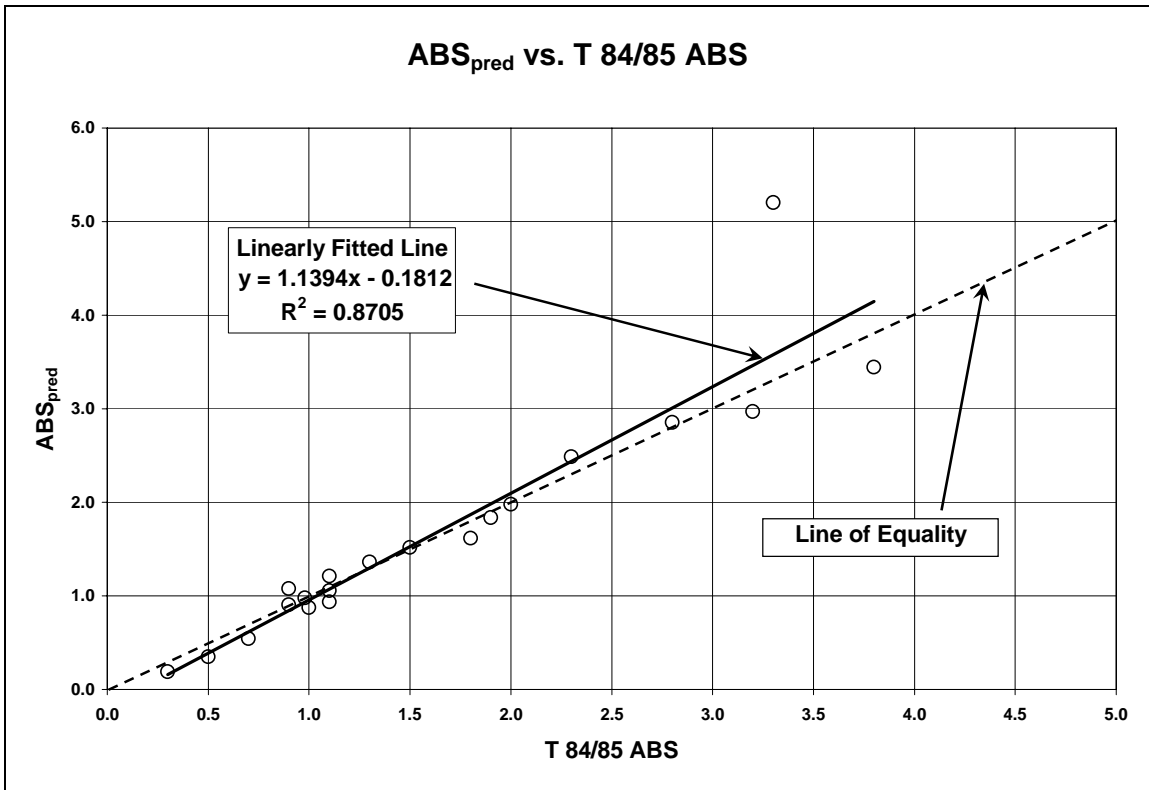


Figure 11: Model Validation: ABS_{pred} vs. T 84/85 ABS

Figures 9 through 11 indicate that the models developed for calibrating the CoreLok method results do a good job of predicting Gsa, Gsb, and ABS values based on an independent dataset, technically speaking, and despite potential outliers. However, the preferred independent dataset would include a larger number of results obtained from different laboratories that use different equipment and operators. It would also include data that reflected the full range of data used in the model development. Requests have been submitted for this type of dataset, but as of this writing have not yet materialized.

Secondary Analysis: Micro-Deval and Los Angeles Abrasion

In an attempt to discover other factors that could be used as predictor variables in the calibration of the CoreLok method to T 84/85 test results, Micro-Deval and Los Angeles Abrasion (LAA) data generally associated with the aggregate samples contained in the dataset supplied by MoDOT were analyzed. The thought was that Micro-Deval and LAA test results were indicators of the mineralogy and internal structure of the aggregates and might help distinguish between different materials. The correlation matrix of the analysis is given below in Table 3. There were only 161 samples with LAA data while there were 169 samples for all other variables. The variable Fines was withheld from the matrix for space-saving purposes and because it did not significantly correlate with Micro-Deval (MicD) and LAA. Those correlations significant at the $\alpha = 0.05$ level are bolded.

Table 3: Correlation Matrix: Micro-Deval & Los Angeles Abrasion as Variables

| Variable | Statistic | Gsb | Gsa | ABS | CorGsb | CorGsa | CorABS | MicD |
|----------|-----------|---------------|---------------|--------------|---------------|---------------|--------------|--------------|
| Gsa | Pearson* | 0.929 | | | | | | |
| | p-value | 0.000 | | | | | | |
| ABS | Pearson* | -0.350 | 0.014 | | | | | |
| | p-value | 0.000 | 0.852 | | | | | |
| CorGsb | Pearson* | 0.959 | 0.987 | -0.094 | | | | |
| | p-value | 0.000 | 0.000 | 0.227 | | | | |
| CorGsa | Pearson* | 0.911 | 0.994 | 0.047 | 0.979 | | | |
| | p-value | 0.000 | 0.000 | 0.544 | 0.000 | | | |
| CorABS | Pearson* | -0.081 | 0.189 | 0.688 | 0.057 | 0.256 | | |
| | p-value | 0.295 | 0.014 | 0.000 | 0.462 | 0.001 | | |
| MicD | Pearson* | -0.418 | -0.251 | 0.488 | -0.310 | -0.238 | 0.321 | |
| | p-value | 0.000 | 0.001 | 0.000 | 0.000 | 0.002 | 0.000 | |
| LAA | Pearson* | -0.183 | 0.086 | 0.323 | 0.025 | 0.147 | 0.211 | 0.629 |
| | p-value | 0.020 | 0.276 | 0.000 | 0.753 | 0.062 | 0.007 | 0.000 |

*Pearson product moment correlation coefficient

Most striking is the fact that Micro-Deval has significant correlation with all the other variables with the strongest being with LAA and the next strongest with ABS. The strong correlation with LAA is intuitive being that both tests are aggregate durability indicators and are similar in concept except that Micro-Deval is defined as percent loss in the presence of water. The correlation with ABS is also somewhat expected in that the pore structure of an aggregate has a direct effect on its absorption and if the volume of pores increases (i.e. absorptive capacity increases), the percent loss of the solids due to abrasion in the presence of water would be expected to increase as well.

Although the resultant models are not presented here, some regression analyses were performed using Micro-Deval as a predictor variable with good results. For example, a linear least squares model that predicted Gsb utilizing CorGsb and Micro-Deval as predictor variables resulted in an $R^2_{\text{pred}} = 0.9316$. This is not quite as good as Equation 8 but is significantly better than the alternate Gsb predictive model shown in Equation 9. The statistics were also very good in the CorGsb and Micro-Deval based model in that all p-values were <0.0001 and the VIF values were 1.1 for the predictors. Therefore, one could argue that this was a productive exercise and warrants further investigation.

CONCLUSIONS

- The following associated aggregate properties are listed in order of decreasing correlation. The ranking is consistent with American Association of State Highway and Transportation Officials (AASHTO) and American Society for Testing and Materials (ASTM) single-operator precision statements for the standard test method results.
 - Non-corrected CoreLok apparent specific gravity (CorGsa) and T 84/85 apparent specific gravity (Gsa)
 - Non-corrected CoreLok bulk specific gravity (CorGsb) and T 84/85 bulk specific gravity (Gsb).
 - Non-corrected CoreLok absorption (CorABS) and T 84/85 absorption (ABS).
- The recommended T 84/85 apparent specific gravity predictive model ($G_{sa_{pred}} = \text{corrected CorGsa}$) is given in Equation 7 and is a function of CorGsa and CorABS with an $R^2_{pred} = 0.9641$. CorABS is the calculated absorption based on CorGsa and CorGsb.
- The recommended T 84/85 bulk specific gravity predictive model ($G_{sb_{pred}} = \text{corrected CorGsb}$) is given in Equation 8 and is a function of CorGsb and ABS with an $R^2_{pred} = 0.9598$. Alternatively, if ABS is not available, $G_{sb_{pred-alt}}$ can be obtained as shown in Equation 9 with a resultant $R^2_{pred} = 0.9047$ using CorABS as a substitute for ABS.
- The recommended T 84/85 absorption predictive model ($ABS_{pred} = \text{corrected CorABS}$) is calculated using the form shown in Equation 5 but is a function of $G_{sa_{pred}}$ and $G_{sb_{pred}}$ with an $R^2_{pred} = 0.9412$. Alternatively when ABS is not available, $ABS_{pred-alt}$ can be obtained with a resultant $R^2_{pred} = 0.5007$ by using $G_{sb_{pred-alt}}$ in place of $G_{sb_{pred}}$ and applying Equation 5.
- A secondary analysis suggests that the aggregate durability tests Micro-Deval and Los Angeles Abrasion have statistically significant correlations to Gsb and ABS with Micro-Deval being the more significant of the two. Findings are of a preliminary nature due to the less-than-perfect association of the Micro-Deval and Los Angeles Abrasion values to the specific samples in the dataset.
- Caution is recommended when applying the predictive models to high specific gravity aggregates ($G_{sa} > 2.900$) due to the very small number of porphyry and steel slag samples in the dataset used during model development.

IMPLEMENTATION

There are two basic scenarios to consider when setting up the CoreLok method worksheet: 1) having performed T 84/85 tests in tandem with or prior to the CoreLok method and therefore knowing the ABS value for that sample and 2) not having ABS thereby depending on the calculated CorABS as an input to the appropriate predictive model in lieu of ABS. The worksheet could be set up in much the same way as the one currently being used by MoDOT. Inputs would be the weight determinations obtained during the CoreLok testing, specific gravity of the bags and rubber sheets, columns for calculating CorGsa, CorGsb, and CorABS, a column for entering T 84/85 ABS, and the columns for calculating $G_{sa_{pred}}$ (CoreLok apparent), $G_{sb_{pred}}$ (CoreLok bulk), and ABS_{pred} (CoreLok absorption) that contain the appropriate predictive models (recommended and alternate, if applicable) with IF statements that can detect whether ABS has been input (e.g. IF ABS is input, use Equation X, otherwise Equation Y).

Based on discussions with MoDOT, most of the time there will be companion T 84/85 values to the CoreLok results that would range from current to historical in terms of age relative to performance of the CoreLok tests. In this case, one would be prudent to periodically check the predicted values output in the worksheet with these companion T 84/85 values, especially for the high specific gravity materials.

SUGGESTED FOLLOW-UP WORK

The primary recommendation is to continue to gather associated CoreLok, T 84/85, Micro-Deval, Los Angeles Abrasion, Sulfate Soundness, Water-Alcohol Freeze, and any other test results that might help characterize the mineralogy, pore structure, or general geology of aggregates used in Missouri. Especially needed is more data for the high specific gravity materials in order to fill in the gap between Gsa values of approximately 2.800 to 3.800. Once a larger and more complete database is established, another look at refining the predictive models would be advantageous.

APPENDIX

Table 4: 180 Sample Dataset Part 1

| SAMPLE ID | FINES | CORTEST | AASHTO | GSB | GSA | ABS | CORGSB | CORGSA | CORABS | LAA | MICD |
|-----------|-------|---------|--------|-------|-------|-----|--------|--------|--------|------|------|
| 17ACG080 | 0 | 0 | T85 | 2.518 | 2.651 | 2.0 | 2.498 | 2.660 | 2.4 | 30.3 | 20.6 |
| 18MA0005 | 0 | 0 | T85 | 2.533 | 2.693 | 2.3 | 2.574 | 2.672 | 1.4 | 21.0 | 10.1 |
| 20MA0379 | 0 | 0 | T85 | 2.678 | 2.720 | 0.6 | 2.720 | 2.759 | 0.5 | 23.0 | 7.6 |
| 20MA0426 | 0 | 0 | T85 | 2.614 | 2.648 | 0.5 | 2.636 | 2.654 | 0.3 | 16.0 | 1.4 |
| 20MA0470 | 1 | 1 | T84 | 2.623 | 2.647 | 0.3 | 2.632 | 2.651 | 0.3 | 19.6 | 1.3 |
| 20MA0553 | 1 | 1 | T85 | 2.715 | 2.801 | 1.1 | 2.789 | 2.813 | 0.3 | 27.8 | 10.5 |
| 20MA0553 | 0 | 0 | T85 | 2.715 | 2.801 | 1.1 | 2.779 | 2.813 | 0.4 | 27.8 | 10.5 |
| 20MA0554 | 1 | 1 | T84 | 2.528 | 2.649 | 1.8 | 2.600 | 2.645 | 0.7 | 20.2 | 2.5 |
| 20MA0555 | 0 | 0 | T85 | 2.755 | 2.812 | 0.7 | 2.794 | 2.825 | 0.4 | 24.0 | 9.2 |
| 20MA0555 | 1 | 1 | T85 | 2.755 | 2.812 | 0.7 | 2.802 | 2.822 | 0.2 | 24.0 | 9.2 |
| 20MA0634 | 0 | 0 | T85 | 2.772 | 2.847 | 0.9 | 2.822 | 2.868 | 0.6 | 22.0 | 6.9 |
| 20MA0635 | 0 | 0 | T85 | 2.743 | 2.831 | 1.1 | 2.811 | 2.858 | 0.6 | 22.0 | 6.9 |
| 20MA0635 | 1 | 1 | T85 | 2.743 | 2.831 | 1.1 | 2.821 | 2.858 | 0.5 | 22.0 | 6.9 |
| 21MA2218 | 0 | 0 | T85 | 2.479 | 2.696 | 3.2 | 2.639 | 2.720 | 1.1 | 28.0 | 22.9 |
| 21MA2229 | 1 | 1 | T84 | 2.628 | 2.645 | 0.2 | 2.631 | 2.642 | 0.2 | | |
| 21MA2230 | 0 | 0 | T85 | 2.448 | 2.680 | 3.5 | 2.620 | 2.709 | 1.3 | 32.7 | 24.3 |
| 21MA2334 | 1 | 1 | T84 | 2.616 | 2.655 | 0.6 | 2.646 | 2.658 | 0.2 | | |
| 21MA2537 | 0 | 0 | T85 | 2.566 | 2.732 | 2.4 | 2.674 | 2.766 | 1.2 | 25.0 | 14.4 |
| 21MA2676 | 0 | 0 | T85 | 2.588 | 2.715 | 1.8 | 2.655 | 2.719 | 0.9 | 23.0 | 18.8 |
| 21MA2680 | 0 | 0 | T85 | 2.573 | 2.715 | 2.0 | 2.667 | 2.728 | 0.8 | 23.0 | 18.8 |
| 22CRS053 | 0 | 0 | T85 | 2.538 | 2.730 | 2.8 | 2.624 | 2.752 | 1.8 | 22.0 | 20.0 |
| 22CRS054 | 0 | 0 | T85 | 2.551 | 2.746 | 2.8 | 2.669 | 2.764 | 1.3 | 22.0 | 20.0 |
| 22DLW186 | 1 | 1 | T85 | 2.482 | 2.750 | 2.5 | 2.656 | 2.776 | 1.6 | 21.0 | 26.7 |
| 22DLW186 | 0 | 0 | T85 | 2.482 | 2.750 | 2.5 | 2.645 | 2.779 | 1.8 | 21.0 | 26.7 |
| 23MA0172 | 1 | 1 | T84 | 2.620 | 2.662 | 0.6 | 2.663 | 2.669 | 0.1 | | 4.0 |
| 23MA0180 | 0 | 0 | T85 | 2.628 | 2.740 | 1.5 | 2.716 | 2.746 | 0.4 | 23.0 | 13.5 |
| 23MA0242 | 1 | 1 | T85 | 2.630 | 2.716 | 1.2 | 2.641 | 2.708 | 0.9 | 24.0 | 13.9 |
| 23MA0242 | 0 | 0 | T85 | 2.630 | 2.716 | 1.2 | 2.697 | 2.719 | 0.3 | 24.0 | 13.9 |
| 23MA0410 | 0 | 0 | T85 | 2.681 | 2.742 | 0.8 | 2.725 | 2.749 | 0.3 | 23.0 | 13.5 |
| 23MA0411 | 0 | 0 | T85 | 2.695 | 2.741 | 0.6 | 2.727 | 2.748 | 0.3 | 23.0 | 13.5 |
| 23MA0412 | 0 | 0 | T85 | 2.668 | 2.742 | 1.0 | 2.731 | 2.751 | 0.3 | 23.0 | 13.5 |
| 23MA0412 | 1 | 1 | T85 | 2.668 | 2.742 | 1.0 | 2.716 | 2.743 | 0.4 | 23.0 | 13.5 |
| 23MA0413 | 0 | 0 | T85 | 2.612 | 2.744 | 1.8 | 2.719 | 2.757 | 0.5 | 23.0 | 13.5 |
| 24GEB006 | 0 | 0 | T85 | 3.202 | 3.511 | 2.7 | 3.415 | 3.626 | 1.7 | | |
| 24GEB011 | 0 | 0 | T85 | 2.587 | 2.707 | 1.7 | 2.654 | 2.720 | 0.9 | 27.0 | 18.6 |
| 24GEB012 | 0 | 0 | T85 | 2.532 | 2.703 | 2.5 | 2.651 | 2.726 | 1.0 | 27.0 | 18.6 |
| 24J3S030 | 0 | 0 | T85 | 2.519 | 2.706 | 2.7 | 2.639 | 2.737 | 1.3 | 29.0 | 25.4 |
| 24J3S031 | 0 | 0 | T85 | 2.496 | 2.716 | 3.2 | 2.659 | 2.745 | 1.2 | 29.0 | 25.4 |
| 24J3S033 | 1 | 1 | T84 | 2.546 | 2.663 | 1.7 | 2.636 | 2.673 | 0.5 | 19.1 | 3.8 |
| 25B2W191 | 1 | 1 | T85 | 2.621 | 2.767 | 2.0 | 2.717 | 2.798 | 1.1 | 30.0 | 14.0 |
| 25B2W191 | 0 | 0 | T85 | 2.621 | 2.767 | 2.0 | 2.736 | 2.802 | 0.9 | 30.0 | 14.0 |
| 25RAK116 | 0 | 0 | T85 | 2.631 | 2.709 | 1.1 | 2.689 | 2.722 | 0.4 | 36.0 | 19.7 |
| 25RAK118 | 0 | 0 | T85 | 2.632 | 2.706 | 1.0 | 2.692 | 2.715 | 0.3 | 36.0 | 19.7 |
| 25RAK120 | 1 | 1 | T84 | 2.529 | 2.657 | 1.9 | 2.592 | 2.650 | 0.8 | | |
| 25RAK183 | 0 | 0 | T85 | 2.629 | 2.698 | 1.0 | 2.691 | 2.712 | 0.3 | 36.0 | 19.7 |
| 25RAK184 | 0 | 0 | T85 | 2.603 | 2.698 | 1.4 | 2.683 | 2.712 | 0.4 | 36.0 | 19.7 |
| 25RAK184 | 1 | 1 | T85 | 2.603 | 2.698 | 1.4 | 2.649 | 2.665 | 0.2 | 36.0 | 19.7 |
| 25RAK186 | 0 | 0 | T85 | 2.600 | 2.700 | 1.4 | 2.691 | 2.709 | 0.3 | 36.0 | 19.7 |
| 26LRB015 | 0 | 0 | T85 | 2.624 | 2.702 | 1.1 | 2.657 | 2.717 | 0.8 | 24.6 | 15.3 |
| 26LRB017 | 0 | 0 | T85 | 2.639 | 2.726 | 1.2 | 2.708 | 2.738 | 0.4 | 26.5 | 15.9 |
| 26LRB035 | 0 | 0 | T85 | 2.589 | 2.729 | 2.0 | 2.692 | 2.740 | 0.7 | 27.0 | 15.9 |
| 26LRB037 | 0 | 0 | T85 | 2.646 | 2.719 | 1.0 | 2.693 | 2.731 | 0.5 | 24.0 | 13.1 |
| 26LRB037 | 1 | 1 | T85 | 2.646 | 2.719 | 1.0 | 2.695 | 2.723 | 0.4 | 24.0 | 13.1 |
| 26MRH294 | 0 | 0 | T85 | 2.550 | 2.695 | 2.1 | 2.653 | 2.726 | 1.0 | 23.2 | 17.1 |
| 26MRH295 | 0 | 0 | T85 | 2.542 | 2.697 | 2.3 | 2.653 | 2.726 | 1.0 | 23.2 | 17.1 |
| 26R2S048 | 0 | 0 | T85 | 2.633 | 2.661 | 0.4 | 2.656 | 2.663 | 0.1 | 16.0 | 1.4 |
| 26R2S048 | 1 | 1 | T85 | 2.633 | 2.661 | 0.4 | 2.651 | 2.658 | 0.1 | 16.0 | 1.4 |
| 26R2S089 | 0 | 0 | T85 | 2.537 | 2.704 | 2.4 | 2.656 | 2.729 | 1.0 | 23.2 | 17.1 |
| 26R2S090 | 0 | 0 | T85 | 2.541 | 2.701 | 2.3 | 2.653 | 2.728 | 1.0 | 23.2 | 17.1 |
| 26R2S106 | 1 | 1 | T84 | 2.621 | 2.650 | 0.4 | 2.638 | 2.646 | 0.1 | | |

Table 5: 180 Sample Dataset Part 2

| SAMPLE ID | FINES | CORTEST | AASHTO | GSB | GSA | ABS | CORGSB | CORGSA | CORABS | LAA | MICD |
|--------------|-------|---------|--------|-------|-------|-----|--------|--------|--------|------|------|
| 26R2S156 | 0 | 0 | T85 | 2.509 | 2.694 | 2.7 | 2.630 | 2.722 | 1.3 | 31.0 | 21.7 |
| 26R2S157 | 0 | 0 | T85 | 2.460 | 2.707 | 3.7 | 2.646 | 2.731 | 1.2 | 31.0 | 21.7 |
| 26R2S159 | 1 | 1 | T84 | 2.622 | 2.647 | 0.4 | 2.632 | 2.649 | 0.3 | | |
| 26R2S163 | 1 | 1 | T85 | 2.592 | 2.734 | 2.0 | 2.704 | 2.755 | 0.7 | 26.5 | 15.9 |
| 26R2S163 | 0 | 0 | T85 | 2.592 | 2.734 | 2.0 | 2.685 | 2.743 | 0.8 | 26.5 | 15.9 |
| 28MA0057 | 1 | 1 | T84 | 2.502 | 2.638 | 2.1 | 2.601 | 2.660 | 0.9 | | 5.6 |
| 28MA0058 | 0 | 0 | T85 | 2.592 | 2.699 | 1.5 | 2.673 | 2.701 | 0.4 | 29.0 | 15.9 |
| 28MA0059 | 0 | 0 | T85 | 2.586 | 2.691 | 1.5 | 2.677 | 2.700 | 0.3 | 29.0 | 15.9 |
| 28MA0077 | 0 | 0 | T85 | 2.638 | 2.694 | 0.8 | 2.653 | 2.675 | 0.3 | 25.0 | 20.4 |
| 28MA0078 | 0 | 0 | T85 | 2.628 | 2.695 | 0.9 | 2.674 | 2.688 | 0.2 | 25.0 | 20.4 |
| 28MA0080 | 0 | 0 | T85 | 2.632 | 2.704 | 1.0 | 2.686 | 2.702 | 0.2 | 25.0 | 20.4 |
| 28MA0080 | 1 | 1 | T85 | 2.632 | 2.704 | 1.0 | 2.680 | 2.702 | 0.3 | 25.0 | 20.4 |
| 28MA0081 | 0 | 0 | T85 | 2.627 | 2.701 | 1.0 | 2.686 | 2.704 | 0.2 | 25.0 | 20.4 |
| 28MA0081 | 1 | 1 | T85 | 2.627 | 2.701 | 1.0 | 2.687 | 2.695 | 0.1 | 25.0 | 20.4 |
| 28MA0095 | 0 | 0 | T85 | 2.640 | 2.796 | 2.1 | 2.728 | 2.819 | 1.2 | 27.5 | 18.6 |
| 28MA0095(A) | 0 | 0 | T85 | 2.640 | 2.796 | 2.1 | 2.740 | 2.823 | 1.1 | 27.5 | 18.6 |
| 28MA0095(B) | 0 | 0 | T85 | 2.634 | 2.794 | 2.2 | 2.728 | 2.819 | 1.2 | 27.5 | 18.6 |
| 28MA0096 | 0 | 0 | T85 | 2.613 | 2.801 | 2.6 | 2.743 | 2.826 | 1.1 | 27.5 | 18.6 |
| 28MA0097 | 0 | 0 | T85 | 2.597 | 2.794 | 2.7 | 2.740 | 2.821 | 1.1 | 27.5 | 18.6 |
| 28MA0097 | 1 | 1 | T85 | 2.597 | 2.794 | 2.7 | 2.742 | 2.813 | 0.9 | 27.5 | 18.6 |
| 28MA0105 | 1 | 1 | T84 | 2.402 | 2.645 | 3.8 | 2.552 | 2.645 | 1.4 | | |
| 28MA0111 | 0 | 0 | T85 | 2.622 | 2.697 | 1.1 | 2.684 | 2.688 | 0.1 | 25.0 | 20.4 |
| 28MA0112 | 1 | 0 | T85 | 2.594 | 2.703 | 1.6 | 2.674 | 2.680 | 0.1 | 25.0 | 20.4 |
| 28MA0192 | 1 | 0 | T85 | 2.616 | 2.698 | 1.2 | 2.681 | 2.692 | 0.2 | 25.0 | 20.4 |
| 29DWM026 | 1 | 1 | T84 | 2.620 | 2.643 | 0.3 | 2.639 | 2.651 | 0.2 | 19.6 | 1.3 |
| 29KVT020 | 0 | 0 | T85 | 2.569 | 2.775 | 2.9 | 2.717 | 2.815 | 1.3 | 30.0 | 16.7 |
| 29KVT051 | 0 | 0 | T85 | 2.608 | 2.790 | 2.5 | 2.731 | 2.821 | 1.2 | 30.0 | 16.7 |
| 29KVT053 | 0 | 0 | T85 | 2.534 | 2.806 | 3.8 | 2.754 | 2.824 | 0.9 | 30.0 | 16.7 |
| 29KVT066 | 0 | 0 | T85 | 2.625 | 2.785 | 2.2 | 2.718 | 2.820 | 1.3 | 30.0 | 16.7 |
| 29KVT067 | 0 | 0 | T85 | 2.552 | 2.770 | 3.1 | 2.688 | 2.819 | 1.7 | 30.0 | 16.7 |
| 29KVT068 | 0 | 0 | T85 | 2.549 | 2.792 | 3.4 | 2.725 | 2.812 | 1.1 | 30.0 | 16.7 |
| 29MLD100 | 0 | 0 | T85 | 2.754 | 2.812 | 0.8 | 2.798 | 2.824 | 0.3 | 25.0 | 11.8 |
| 29MLD101 | 0 | 0 | T85 | 2.709 | 2.816 | 1.4 | 2.792 | 2.824 | 0.4 | 25.0 | 11.8 |
| 29MLD196 | 0 | 0 | T85 | 2.735 | 2.807 | 0.9 | 2.800 | 2.822 | 0.3 | 25.0 | 11.8 |
| 29MLD197 | 0 | 0 | T85 | 2.760 | 2.808 | 0.6 | 2.789 | 2.820 | 0.4 | 25.0 | 11.8 |
| 2MFO0076 | 0 | 0 | T85 | 2.613 | 2.789 | 2.4 | 2.728 | 2.819 | 1.2 | 27.5 | 18.6 |
| 2MFO0078 | 0 | 0 | T85 | 2.627 | 2.690 | 0.9 | 2.672 | 2.687 | 0.2 | 25.0 | 20.4 |
| 30MA0334 | 0 | 0 | T85 | 2.682 | 2.804 | 1.6 | 2.793 | 2.851 | 0.7 | 22.4 | 9.0 |
| 33MA0155 | 0 | 0 | T85 | 2.494 | 2.696 | 3.0 | 2.652 | 2.722 | 1.0 | 38.0 | 23.3 |
| 34SDS066 | 0 | 0 | T85 | 2.566 | 2.716 | 2.2 | 2.690 | 2.722 | 0.4 | 26.0 | 16.4 |
| 34SDS115 | 0 | 0 | T85 | 2.607 | 2.705 | 1.4 | 2.675 | 2.721 | 0.6 | 27.0 | 18.6 |
| 34SDS116 | 0 | 0 | T85 | 2.581 | 2.709 | 1.8 | 2.691 | 2.724 | 0.5 | 27.0 | 18.6 |
| 34SDS236 | 0 | 0 | T85 | 3.442 | 3.638 | 1.6 | 3.623 | 3.747 | 0.9 | | |
| 35DGG008 | 0 | 0 | T85 | 2.632 | 2.781 | 2.0 | 2.746 | 2.809 | 0.8 | 30.0 | 14.0 |
| 36JEC100 | 0 | 0 | T85 | 2.550 | 2.712 | 2.3 | 2.660 | 2.737 | 1.0 | 26.5 | 15.9 |
| 36JEC101 | 0 | 0 | T85 | 2.534 | 2.729 | 2.8 | 2.692 | 2.739 | 0.6 | 26.5 | 15.9 |
| 36JEC109 | 0 | 0 | T85 | 2.612 | 2.705 | 1.3 | 2.667 | 2.720 | 0.7 | 24.6 | 15.3 |
| 36LRB054 | 0 | 0 | T85 | 2.631 | 2.710 | 1.1 | 2.685 | 2.717 | 0.4 | 27.0 | 14.5 |
| 36LRB070 | 0 | 0 | T85 | 2.542 | 2.715 | 2.5 | 2.655 | 2.735 | 1.1 | 24.0 | 22.5 |
| 36LRB071 | 0 | 0 | T85 | 2.480 | 2.724 | 3.6 | 2.683 | 2.726 | 0.6 | 24.0 | 22.5 |
| 37TRJ199 | 0 | 0 | T85 | 2.625 | 2.696 | 0.9 | 2.620 | 2.681 | 0.9 | 21.0 | 8.3 |
| 37TRJ201 | 0 | 0 | T85 | 2.567 | 2.670 | 1.5 | 2.627 | 2.671 | 0.6 | 21.0 | 8.3 |
| 37TRJ202 | 0 | 0 | T85 | 2.521 | 2.647 | 1.8 | 2.606 | 2.654 | 0.7 | 21.0 | 8.3 |
| 39KVT046 | 0 | 0 | T85 | 2.692 | 2.791 | 1.3 | 2.773 | 2.803 | 0.4 | 22.0 | 9.4 |
| 39MLD045 | 0 | 0 | T85 | 2.696 | 2.804 | 1.4 | 2.798 | 2.812 | 0.2 | 25.0 | 11.8 |
| 40MA0192 | 1 | 0 | T85 | 2.599 | 2.650 | 0.7 | 2.638 | 2.648 | 0.1 | 16.0 | 1.4 |
| 40MA0523(B1) | 0 | 0 | T85 | 2.676 | 2.786 | 1.5 | 2.721 | 2.776 | 0.7 | | |
| 40MA0524(B2) | 0 | 0 | T85 | 2.685 | 2.755 | 1.0 | 2.718 | 2.750 | 0.4 | | |
| 40MA0527(B4) | 1 | 1 | AVG | 2.693 | 2.766 | 1.0 | 2.718 | 2.759 | 0.5 | | |
| 40MA0572 | 0 | 0 | T85 | 2.631 | 2.646 | 0.2 | 2.649 | 2.655 | 0.1 | 16.0 | 1.4 |

Table 6: 180 Sample Dataset Part 3

| SAMPLE ID | FINES | CORTEST | AASHTO | GSB | GSA | ABS | CORGSB | CORGSA | CORABS | LAA | MICD |
|---------------|-------|---------|--------|-------|-------|-----|--------|--------|--------|------|------|
| 41MA2281 | 0 | 0 | T85 | 2.571 | 2.731 | 2.0 | 2.658 | 2.720 | 0.9 | 25.0 | 19.4 |
| 41MA2334 | 0 | 0 | T85 | 2.602 | 2.641 | 0.6 | 2.651 | 2.658 | 0.1 | 19.4 | 2.8 |
| 41MA2339 | 0 | 0 | T85 | 2.514 | 2.694 | 2.7 | 2.621 | 2.719 | 1.4 | 28.0 | 22.9 |
| 41MA2340 | 0 | 0 | T85 | 2.466 | 2.702 | 3.5 | 2.641 | 2.725 | 1.2 | 28.0 | 22.9 |
| 41MA2389 | 1 | 0 | T85 | 2.611 | 2.740 | 1.8 | 2.684 | 2.735 | 0.7 | 22.6 | 14.5 |
| 42JPS032 | 0 | 0 | T85 | 2.528 | 2.734 | 3.0 | 2.666 | 2.755 | 1.2 | 22.0 | 20.0 |
| 42JPS063 | 0 | 0 | T85 | 2.535 | 2.741 | 3.0 | 2.688 | 2.739 | 0.7 | 22.0 | 20.0 |
| 42JSP042 | 0 | 0 | T85 | 2.569 | 2.736 | 2.4 | 2.660 | 2.747 | 1.2 | 22.0 | 20.0 |
| 44GEB002 | 1 | 0 | T85 | 2.592 | 2.707 | 1.6 | 2.659 | 2.721 | 0.8 | 27.0 | 18.6 |
| 44GEB002 | 1 | 0 | T85 | 2.772 | 2.847 | 0.9 | 2.659 | 2.721 | 0.8 | | |
| 44GEB033 | 0 | 0 | T85 | 3.556 | 3.721 | 1.2 | 3.703 | 3.808 | 0.7 | | |
| 44SDS045 | 0 | 0 | T85 | 2.589 | 2.704 | 1.6 | 2.650 | 2.715 | 0.9 | 27.0 | 18.6 |
| 44SDS046 | 0 | 0 | T85 | 2.575 | 2.702 | 1.8 | 2.660 | 2.720 | 0.8 | 27.0 | 18.6 |
| 44SDS047 | 0 | 0 | T85 | 2.562 | 2.716 | 2.2 | 2.682 | 2.720 | 0.5 | 27.0 | 18.6 |
| 45B2W078 | 1 | 0 | T85 | 2.760 | 2.808 | 0.6 | 2.757 | 2.822 | 0.8 | | |
| 45B2W078 | 1 | 0 | T85 | 2.691 | 2.777 | 1.1 | 2.750 | 2.822 | 0.9 | 32.5 | 13.8 |
| 45DGG114 | 0 | 0 | T85 | 2.654 | 2.713 | 0.8 | 2.693 | 2.714 | 0.3 | 23.9 | 15.1 |
| 45DGG115 | 0 | 0 | T85 | 2.627 | 2.716 | 1.3 | 2.710 | 2.726 | 0.2 | 23.9 | 15.1 |
| 45JDR206 | 0 | 0 | T85 | 2.431 | 2.609 | 2.8 | 2.531 | 2.639 | 1.6 | 17.0 | 1.7 |
| 45JDR225 | 1 | 0 | T85 | 2.429 | 2.602 | 2.7 | 2.602 | 2.639 | 0.5 | | |
| 45JDR225 | 1 | 0 | T85 | 2.754 | 2.812 | 0.8 | 2.543 | 2.639 | 1.4 | | |
| 45TMS137 | 1 | 0 | T85 | 2.627 | 2.690 | 0.9 | 2.708 | 2.736 | 0.4 | | |
| 45TMS137 | 1 | 0 | T85 | 2.624 | 2.731 | 1.5 | 2.708 | 2.736 | 0.4 | 23.9 | 17.3 |
| 45TMS137 | 1 | 0 | T85 | 2.681 | 2.742 | 0.8 | 2.688 | 2.740 | 0.7 | | |
| 45TMS155 | 0 | 0 | T85 | 2.635 | 2.731 | 1.3 | 2.675 | 2.734 | 0.8 | 16.0 | 1.4 |
| 45TMS156 | 0 | 0 | T85 | 2.625 | 2.734 | 1.5 | 2.705 | 2.747 | 0.6 | 16.0 | 1.4 |
| 45TMS163 | 1 | 0 | T85 | 2.735 | 2.807 | 0.9 | 2.691 | 2.720 | 0.4 | | |
| 45TMS163 | 1 | 0 | T85 | 2.599 | 2.698 | 1.4 | 2.692 | 2.720 | 0.4 | 23.9 | 17.3 |
| 45TMS174 | 1 | 0 | T85 | 2.617 | 2.651 | 0.5 | 2.757 | 2.835 | 1.0 | | |
| 45TMS174 | 1 | 0 | T85 | 2.613 | 2.797 | 2.5 | 2.757 | 2.835 | 1.0 | 33.0 | 19.0 |
| 45TMS175 | 1 | 0 | T85 | 2.617 | 2.651 | 0.5 | 2.736 | 2.825 | 1.2 | | |
| 45TMS175 | 1 | 0 | T85 | 2.608 | 2.782 | 2.4 | 2.736 | 2.825 | 1.1 | 33.0 | 19.0 |
| 45TMS176 | 1 | 0 | T85 | 2.563 | 2.802 | 2.7 | 2.759 | 2.829 | 0.9 | 33.0 | 19.0 |
| 45TMS176 | 1 | 0 | T85 | 2.678 | 2.720 | 0.6 | 2.759 | 2.829 | 0.9 | | |
| 46LRB066 | 0 | 0 | T85 | 2.565 | 2.703 | 2.0 | 2.662 | 2.720 | 0.8 | 23.2 | 17.1 |
| 48MA0039 | 1 | 0 | T85 | 2.522 | 2.645 | 1.8 | 2.598 | 2.631 | 0.5 | 19.1 | 3.8 |
| 48MA0105 | 1 | 0 | T85 | 2.695 | 2.741 | 0.6 | 2.630 | 2.636 | 0.1 | | |
| 48MA0105 | 1 | 0 | T85 | 2.579 | 2.626 | 0.7 | 2.630 | 2.636 | 0.1 | 24.5 | 2.9 |
| 48MA0108 | 1 | 0 | T85 | 2.577 | 2.690 | 1.6 | 2.664 | 2.698 | 0.5 | 29.0 | 15.9 |
| 48MA0108 | 1 | 0 | T85 | 2.617 | 2.651 | 0.5 | 2.663 | 2.698 | 0.5 | | |
| 48MA0109 | 1 | 0 | T85 | 2.617 | 2.651 | 0.5 | 2.656 | 2.723 | 0.9 | | |
| 48MA0109 | 1 | 0 | T85 | 2.596 | 2.705 | 1.6 | 2.656 | 2.723 | 0.9 | 29.0 | 15.9 |
| 49KVT080 | 0 | 0 | T85 | 2.579 | 2.791 | 2.9 | 2.744 | 2.819 | 1.0 | 16.0 | 1.4 |
| 49KVT081 | 1 | 0 | T85 | 2.597 | 2.798 | 2.8 | 2.736 | 2.809 | 1.0 | 30.0 | 16.7 |
| 49KVT081 | 0 | 0 | T85 | 2.527 | 2.795 | 3.8 | 2.748 | 2.814 | 0.8 | 30.0 | 16.7 |
| 54SDS080 | 0 | 0 | T85 | 3.534 | 3.695 | 1.2 | 3.768 | 3.956 | 1.3 | | |
| 54SDS081 | 1 | 1 | T85 | 3.534 | 3.695 | 1.2 | 3.624 | 3.827 | 1.5 | | |
| 55J2D008(C3) | 1 | 1 | T84 | 2.628 | 2.655 | 0.4 | 2.633 | 2.641 | 0.1 | | |
| 55TMS029(C1) | 0 | 0 | T85 | 2.650 | 2.775 | 1.7 | 2.732 | 2.807 | 1.0 | | |
| 55TMS030(C2) | 1 | 0 | AVG | 2.639 | 2.788 | 2.0 | 2.742 | 2.808 | 0.9 | | |
| 57R7S215(A1) | 0 | 0 | T85 | 2.538 | 2.766 | 3.2 | 2.684 | 2.824 | 1.8 | | |
| 57R7S216(AA2) | 1 | 0 | AVG | 2.581 | 2.798 | 3.0 | 2.727 | 2.818 | 1.2 | | |
| 57R7S217(AA4) | 1 | 1 | AVG | 2.584 | 2.797 | 3.0 | 2.735 | 2.821 | 1.1 | | |
| 57R7S218(AA3) | 1 | 0 | AVG | 2.584 | 2.797 | 3.0 | 2.724 | 2.827 | 1.3 | | |
| 69WPM070 | 0 | 0 | T85 | 2.927 | 2.982 | 0.6 | 2.970 | 3.017 | 0.5 | 19.0 | 7.4 |
| 69WPM074 | 0 | 0 | T85 | 2.927 | 2.982 | 0.6 | 2.978 | 3.031 | 0.6 | 19.0 | 7.4 |
| J5I0679 | 0 | 0 | T85 | 2.570 | 2.670 | 1.5 | 2.655 | 2.694 | 0.6 | 38.0 | 19.6 |
| J5P0704 | 1 | 1 | T85 | 2.631 | 2.718 | 1.2 | 2.682 | 2.719 | 0.5 | 23.9 | 17.3 |
| J5P0704 | 0 | 0 | T85 | 2.631 | 2.718 | 1.2 | 2.687 | 2.724 | 0.5 | 23.9 | 17.3 |
| J6U1047 | 1 | 1 | T85 | 2.610 | 2.737 | 1.9 | 2.690 | 2.738 | 0.7 | 26.5 | 15.9 |
| | | | Max | 3.556 | 3.721 | 3.8 | 3.768 | 3.956 | 2.4 | | |
| | | | Min | 2.402 | 2.602 | 0.2 | 2.498 | 2.631 | 0.1 | | |

Table 7: T 84/85 & Predicted Values Part 1

| SAMPLE ID | GSB | | | GSA | | ABS | | |
|-----------|---------|---------------|---------------|---------|---------------|---------|--------------------|--------------------|
| | T 84/85 | Pred.(Eqn. 8) | Pred.(Eqn. 9) | T 84/85 | Pred.(Eqn. 7) | T 84/85 | Pred.(Eqn's 8 & 7) | Pred.(Eqn's 9 & 7) |
| 17ACG080 | 2.518 | 2.425 | 2.406 | 2.651 | 2.617 | 2.0 | 3.0 | 3.4 |
| 18MA0005 | 2.533 | 2.475 | 2.481 | 2.693 | 2.649 | 2.3 | 2.7 | 2.6 |
| 20MA0379 | 2.678 | 2.692 | 2.642 | 2.720 | 2.747 | 0.6 | 0.7 | 1.4 |
| 20MA0426 | 2.614 | 2.623 | 2.596 | 2.648 | 2.656 | 0.5 | 0.5 | 0.9 |
| 20MA0470 | 2.623 | 2.630 | 2.592 | 2.647 | 2.653 | 0.3 | 0.3 | 0.9 |
| 20MA0553 | 2.715 | 2.726 | 2.718 | 2.801 | 2.800 | 1.1 | 1.0 | 1.1 |
| 20MA0553 | 2.715 | 2.717 | 2.698 | 2.801 | 2.798 | 1.1 | 1.1 | 1.3 |
| 20MA0554 | 2.528 | 2.524 | 2.535 | 2.649 | 2.640 | 1.8 | 1.7 | 1.6 |
| 20MA0555 | 2.755 | 2.751 | 2.715 | 2.812 | 2.809 | 0.7 | 0.8 | 1.2 |
| 20MA0555 | 2.755 | 2.758 | 2.735 | 2.812 | 2.809 | 0.7 | 0.7 | 1.0 |
| 20MA0634 | 2.772 | 2.765 | 2.724 | 2.847 | 2.845 | 0.9 | 1.0 | 1.6 |
| 20MA0635 | 2.743 | 2.745 | 2.713 | 2.831 | 2.835 | 1.1 | 1.2 | 1.6 |
| 20MA0635 | 2.743 | 2.754 | 2.733 | 2.831 | 2.838 | 1.1 | 1.1 | 1.4 |
| 21MA2218 | 2.479 | 2.486 | 2.543 | 2.696 | 2.699 | 3.2 | 3.2 | 2.3 |
| 21MA2229 | 2.628 | 2.635 | 2.602 | 2.645 | 2.648 | 0.2 | 0.2 | 0.7 |
| 21MA2230 | 2.448 | 2.453 | 2.523 | 2.680 | 2.686 | 3.5 | 3.5 | 2.4 |
| 21MA2334 | 2.616 | 2.626 | 2.611 | 2.655 | 2.662 | 0.6 | 0.5 | 0.7 |
| 21MA2537 | 2.566 | 2.558 | 2.566 | 2.732 | 2.739 | 2.4 | 2.6 | 2.4 |
| 21MA2676 | 2.588 | 2.573 | 2.567 | 2.715 | 2.703 | 1.8 | 1.9 | 2.0 |
| 21MA2680 | 2.573 | 2.573 | 2.579 | 2.715 | 2.712 | 2.0 | 2.0 | 1.9 |
| 22CRS053 | 2.538 | 2.493 | 2.512 | 2.730 | 2.715 | 2.8 | 3.3 | 3.0 |
| 22CRS054 | 2.551 | 2.533 | 2.561 | 2.746 | 2.736 | 2.8 | 2.9 | 2.5 |
| 22DLW186 | 2.482 | 2.537 | 2.541 | 2.750 | 2.740 | 2.5 | 2.9 | 2.9 |
| 22DLW186 | 2.482 | 2.527 | 2.528 | 2.750 | 2.738 | 2.5 | 3.1 | 3.0 |
| 23MA0172 | 2.620 | 2.641 | 2.635 | 2.662 | 2.673 | 0.6 | 0.5 | 0.5 |
| 23MA0180 | 2.628 | 2.642 | 2.649 | 2.740 | 2.737 | 1.5 | 1.3 | 1.2 |
| 23MA0242 | 2.630 | 2.591 | 2.553 | 2.716 | 2.692 | 1.2 | 1.4 | 2.0 |
| 23MA0242 | 2.630 | 2.640 | 2.641 | 2.716 | 2.715 | 1.2 | 1.0 | 1.0 |
| 23MA0410 | 2.681 | 2.686 | 2.663 | 2.742 | 2.742 | 0.8 | 0.8 | 1.1 |
| 23MA0411 | 2.695 | 2.698 | 2.669 | 2.741 | 2.742 | 0.6 | 0.6 | 1.0 |
| 23MA0412 | 2.668 | 2.681 | 2.674 | 2.742 | 2.745 | 1.0 | 0.9 | 1.0 |
| 23MA0412 | 2.668 | 2.668 | 2.652 | 2.742 | 2.735 | 1.0 | 0.9 | 1.1 |
| 23MA0413 | 2.612 | 2.628 | 2.642 | 2.744 | 2.745 | 1.8 | 1.6 | 1.4 |
| 24GEB006 | 3.202 | 3.191 | 3.215 | 3.511 | 3.512 | 2.7 | 2.9 | 2.6 |
| 24GEB011 | 2.587 | 2.577 | 2.565 | 2.707 | 2.703 | 1.7 | 1.8 | 2.0 |
| 24GEB012 | 2.532 | 2.532 | 2.556 | 2.703 | 2.706 | 2.5 | 2.5 | 2.2 |
| 24J3S030 | 2.519 | 2.512 | 2.535 | 2.706 | 2.710 | 2.7 | 2.9 | 2.5 |
| 24J3S031 | 2.496 | 2.504 | 2.558 | 2.716 | 2.721 | 3.2 | 3.2 | 2.3 |
| 24J3S033 | 2.546 | 2.561 | 2.573 | 2.663 | 2.668 | 1.7 | 1.6 | 1.4 |
| 25B2W191 | 2.621 | 2.616 | 2.608 | 2.767 | 2.771 | 2.0 | 2.1 | 2.3 |
| 25B2W191 | 2.621 | 2.633 | 2.633 | 2.767 | 2.779 | 2.0 | 2.0 | 2.0 |
| 25RAK116 | 2.631 | 2.638 | 2.622 | 2.709 | 2.714 | 1.1 | 1.1 | 1.3 |
| 25RAK118 | 2.632 | 2.646 | 2.636 | 2.706 | 2.711 | 1.0 | 0.9 | 1.1 |
| 25RAK120 | 2.529 | 2.512 | 2.519 | 2.657 | 2.641 | 1.9 | 1.9 | 1.8 |
| 25RAK183 | 2.629 | 2.645 | 2.638 | 2.698 | 2.709 | 1.0 | 0.9 | 1.0 |
| 25RAK184 | 2.603 | 2.617 | 2.621 | 2.698 | 2.706 | 1.4 | 1.3 | 1.2 |
| 25RAK184 | 2.603 | 2.588 | 2.609 | 2.698 | 2.667 | 1.4 | 1.1 | 0.8 |
| 25RAK186 | 2.600 | 2.625 | 2.642 | 2.700 | 2.707 | 1.4 | 1.2 | 0.9 |
| 26LRB015 | 2.624 | 2.611 | 2.571 | 2.702 | 2.703 | 1.1 | 1.3 | 1.9 |
| 26LRB017 | 2.639 | 2.650 | 2.641 | 2.726 | 2.730 | 1.2 | 1.1 | 1.2 |
| 26LRB035 | 2.589 | 2.595 | 2.610 | 2.729 | 2.727 | 2.0 | 1.9 | 1.6 |
| 26LRB037 | 2.646 | 2.647 | 2.621 | 2.719 | 2.721 | 1.0 | 1.0 | 1.4 |
| 26LRB037 | 2.646 | 2.649 | 2.633 | 2.719 | 2.717 | 1.0 | 0.9 | 1.2 |
| 26MRH294 | 2.550 | 2.555 | 2.559 | 2.695 | 2.707 | 2.1 | 2.2 | 2.1 |
| 26MRH295 | 2.542 | 2.545 | 2.559 | 2.697 | 2.707 | 2.3 | 2.4 | 2.1 |
| 26R2S048 | 2.633 | 2.646 | 2.629 | 2.661 | 2.668 | 0.4 | 0.3 | 0.6 |
| 26R2S048 | 2.633 | 2.641 | 2.623 | 2.661 | 2.664 | 0.4 | 0.3 | 0.6 |
| 26R2S089 | 2.537 | 2.542 | 2.561 | 2.704 | 2.709 | 2.4 | 2.4 | 2.1 |
| 26R2S090 | 2.541 | 2.544 | 2.558 | 2.701 | 2.708 | 2.3 | 2.4 | 2.2 |
| 26R2S106 | 2.621 | 2.630 | 2.612 | 2.650 | 2.652 | 0.4 | 0.3 | 0.6 |

Table 8: T 84/85 & Predicted Values Part 2

| SAMPLE ID | GSB | | | GSA | | ABS | | |
|--------------|---------|---------------|---------------|---------|---------------|---------|--------------------|--------------------|
| | T 84/85 | Pred.(Eqn. 8) | Pred.(Eqn. 9) | T 84/85 | Pred.(Eqn. 7) | T 84/85 | Pred.(Eqn's 8 & 7) | Pred.(Eqn's 9 & 7) |
| 26R2S156 | 2.509 | 2.504 | 2.530 | 2.694 | 2.698 | 2.7 | 2.9 | 2.5 |
| 26R2S157 | 2.460 | 2.467 | 2.547 | 2.707 | 2.708 | 3.7 | 3.6 | 2.3 |
| 26R2S159 | 2.622 | 2.625 | 2.593 | 2.647 | 2.652 | 0.4 | 0.4 | 0.9 |
| 26R2S163 | 2.592 | 2.605 | 2.617 | 2.734 | 2.740 | 2.0 | 1.9 | 1.7 |
| 26R2S163 | 2.592 | 2.588 | 2.595 | 2.734 | 2.727 | 2.0 | 2.0 | 1.9 |
| 28MA0057 | 2.502 | 2.510 | 2.525 | 2.638 | 2.650 | 2.1 | 2.1 | 1.9 |
| 28MA0058 | 2.592 | 2.604 | 2.615 | 2.699 | 2.697 | 1.5 | 1.3 | 1.2 |
| 28MA0059 | 2.586 | 2.607 | 2.624 | 2.691 | 2.697 | 1.5 | 1.3 | 1.0 |
| 28MA0077 | 2.638 | 2.623 | 2.605 | 2.694 | 2.675 | 0.8 | 0.7 | 1.0 |
| 28MA0078 | 2.628 | 2.636 | 2.633 | 2.695 | 2.689 | 0.9 | 0.7 | 0.8 |
| 28MA0080 | 2.632 | 2.641 | 2.640 | 2.704 | 2.701 | 1.0 | 0.8 | 0.8 |
| 28MA0080 | 2.632 | 2.636 | 2.628 | 2.704 | 2.700 | 1.0 | 0.9 | 1.0 |
| 28MA0081 | 2.627 | 2.641 | 2.639 | 2.701 | 2.702 | 1.0 | 0.9 | 0.9 |
| 28MA0081 | 2.627 | 2.642 | 2.653 | 2.701 | 2.697 | 1.0 | 0.8 | 0.6 |
| 28MA0095 | 2.640 | 2.621 | 2.613 | 2.796 | 2.788 | 2.1 | 2.3 | 2.4 |
| 28MA0095(A) | 2.640 | 2.631 | 2.626 | 2.796 | 2.794 | 2.1 | 2.2 | 2.3 |
| 28MA0095(B) | 2.634 | 2.616 | 2.613 | 2.794 | 2.788 | 2.2 | 2.4 | 2.4 |
| 28MA0096 | 2.613 | 2.608 | 2.630 | 2.801 | 2.796 | 2.6 | 2.6 | 2.3 |
| 28MA0097 | 2.597 | 2.600 | 2.627 | 2.794 | 2.792 | 2.7 | 2.7 | 2.2 |
| 28MA0097 | 2.597 | 2.602 | 2.635 | 2.794 | 2.787 | 2.7 | 2.6 | 2.1 |
| 28MA0105 | 2.402 | 2.379 | 2.466 | 2.645 | 2.626 | 3.8 | 4.0 | 2.5 |
| 28MA0111 | 2.622 | 2.634 | 2.657 | 2.697 | 2.692 | 1.1 | 0.8 | 0.5 |
| 28MA0112 | 2.594 | 2.600 | 2.646 | 2.703 | 2.684 | 1.6 | 1.2 | 0.5 |
| 28MA0192 | 2.616 | 2.626 | 2.643 | 2.698 | 2.693 | 1.2 | 0.9 | 0.7 |
| 29DWM026 | 2.620 | 2.636 | 2.608 | 2.643 | 2.655 | 0.3 | 0.3 | 0.7 |
| 29KVT020 | 2.569 | 2.570 | 2.600 | 2.775 | 2.782 | 2.9 | 3.0 | 2.5 |
| 29KVT051 | 2.608 | 2.603 | 2.615 | 2.790 | 2.790 | 2.5 | 2.6 | 2.4 |
| 29KVT053 | 2.534 | 2.555 | 2.647 | 2.806 | 2.798 | 3.8 | 3.4 | 2.0 |
| 29KVT066 | 2.625 | 2.607 | 2.599 | 2.785 | 2.786 | 2.2 | 2.5 | 2.6 |
| 29KVT067 | 2.552 | 2.534 | 2.565 | 2.770 | 2.777 | 3.1 | 3.4 | 3.0 |
| 29KVT068 | 2.549 | 2.550 | 2.611 | 2.792 | 2.783 | 3.4 | 3.3 | 2.4 |
| 29MLD100 | 2.754 | 2.749 | 2.724 | 2.812 | 2.810 | 0.8 | 0.8 | 1.1 |
| 29MLD101 | 2.709 | 2.713 | 2.711 | 2.816 | 2.808 | 1.4 | 1.3 | 1.3 |
| 29MLD196 | 2.735 | 2.746 | 2.731 | 2.807 | 2.809 | 0.9 | 0.8 | 1.0 |
| 29MLD197 | 2.760 | 2.752 | 2.710 | 2.808 | 2.805 | 0.6 | 0.7 | 1.3 |
| 2MFO0076 | 2.613 | 2.605 | 2.612 | 2.789 | 2.788 | 2.4 | 2.5 | 2.4 |
| 2MFO0078 | 2.627 | 2.634 | 2.630 | 2.690 | 2.688 | 0.9 | 0.8 | 0.8 |
| 30MA0334 | 2.682 | 2.704 | 2.689 | 2.804 | 2.826 | 1.6 | 1.6 | 1.8 |
| 33MA0155 | 2.494 | 2.508 | 2.561 | 2.696 | 2.704 | 3.0 | 2.9 | 2.1 |
| 34SDS066 | 2.566 | 2.582 | 2.623 | 2.716 | 2.715 | 2.2 | 1.9 | 1.3 |
| 34SDS115 | 2.607 | 2.611 | 2.598 | 2.705 | 2.710 | 1.4 | 1.4 | 1.6 |
| 34SDS116 | 2.581 | 2.604 | 2.622 | 2.709 | 2.716 | 1.8 | 1.6 | 1.3 |
| 34SDS236 | 3.442 | 3.430 | 3.460 | 3.638 | 3.638 | 1.6 | 1.7 | 1.4 |
| 35DGG008 | 2.632 | 2.642 | 2.644 | 2.781 | 2.786 | 2.0 | 2.0 | 1.9 |
| 36JEC100 | 2.550 | 2.551 | 2.563 | 2.712 | 2.716 | 2.3 | 2.4 | 2.2 |
| 36JEC101 | 2.534 | 2.553 | 2.611 | 2.729 | 2.726 | 2.8 | 2.5 | 1.6 |
| 36JEC109 | 2.612 | 2.609 | 2.585 | 2.705 | 2.707 | 1.3 | 1.4 | 1.7 |
| 36LRB054 | 2.631 | 2.635 | 2.620 | 2.710 | 2.710 | 1.1 | 1.1 | 1.3 |
| 36LRB070 | 2.542 | 2.536 | 2.557 | 2.715 | 2.713 | 2.5 | 2.6 | 2.3 |
| 36LRB071 | 2.480 | 2.504 | 2.608 | 2.724 | 2.715 | 3.6 | 3.1 | 1.5 |
| 37TRJ199 | 2.625 | 2.589 | 2.540 | 2.696 | 2.669 | 0.9 | 1.2 | 1.9 |
| 37TRJ201 | 2.567 | 2.563 | 2.559 | 2.670 | 2.664 | 1.5 | 1.5 | 1.5 |
| 37TRJ202 | 2.521 | 2.529 | 2.537 | 2.647 | 2.648 | 1.8 | 1.8 | 1.6 |
| 39KVT046 | 2.692 | 2.702 | 2.697 | 2.791 | 2.790 | 1.3 | 1.2 | 1.2 |
| 39MLD045 | 2.696 | 2.718 | 2.738 | 2.804 | 2.802 | 1.4 | 1.1 | 0.8 |
| 40MA0192 | 2.599 | 2.615 | 2.608 | 2.650 | 2.654 | 0.7 | 0.6 | 0.7 |
| 40MA0523(B1) | 2.676 | 2.648 | 2.629 | 2.786 | 2.758 | 1.5 | 1.5 | 1.8 |
| 40MA0524(B2) | 2.685 | 2.671 | 2.647 | 2.755 | 2.740 | 1.0 | 0.9 | 1.3 |
| 40MA0527(B4) | 2.693 | 2.670 | 2.638 | 2.766 | 2.746 | 1.0 | 1.0 | 1.5 |
| 40MA0572 | 2.631 | 2.650 | 2.625 | 2.646 | 2.661 | 0.2 | 0.2 | 0.5 |

Table 9: T 84/85 & Predicted Values Part 3

| SAMPLE ID | GSB | | | GSA | | ABS | | |
|--------------|---------|---------------|---------------|---------|---------------|---------|--------------------|--------------------|
| | T 84/85 | Pred.(Eqn. 8) | Pred.(Eqn. 9) | T 84/85 | Pred.(Eqn. 7) | T 84/85 | Pred.(Eqn's 8 & 7) | Pred.(Eqn's 9 & 7) |
| 41MA2281 | 2.571 | 2.565 | 2.570 | 2.731 | 2.705 | 2.0 | 2.0 | 1.9 |
| 41MA2334 | 2.602 | 2.631 | 2.625 | 2.641 | 2.663 | 0.6 | 0.5 | 0.5 |
| 41MA2339 | 2.514 | 2.496 | 2.520 | 2.694 | 2.693 | 2.7 | 2.9 | 2.5 |
| 41MA2340 | 2.466 | 2.472 | 2.542 | 2.702 | 2.703 | 3.5 | 3.5 | 2.3 |
| 41MA2389 | 2.611 | 2.598 | 2.600 | 2.740 | 2.722 | 1.8 | 1.8 | 1.7 |
| 42JPS032 | 2.528 | 2.520 | 2.562 | 2.734 | 2.729 | 3.0 | 3.0 | 2.4 |
| 42JPS063 | 2.535 | 2.539 | 2.604 | 2.741 | 2.725 | 3.0 | 2.7 | 1.7 |
| 42JSP042 | 2.569 | 2.546 | 2.557 | 2.736 | 2.723 | 2.4 | 2.6 | 2.4 |
| 44GEB002 | 2.592 | 2.587 | 2.572 | 2.707 | 2.705 | 1.6 | 1.7 | 1.9 |
| 44GEB002 | 2.772 | 2.623 | 2.572 | 2.847 | 2.705 | 0.9 | 1.2 | 1.9 |
| 44GEB033 | 3.556 | 3.521 | 3.558 | 3.721 | 3.697 | 1.2 | 1.4 | 1.1 |
| 44SDS045 | 2.589 | 2.578 | 2.561 | 2.704 | 2.699 | 1.6 | 1.7 | 2.0 |
| 44SDS046 | 2.575 | 2.577 | 2.573 | 2.702 | 2.705 | 1.8 | 1.8 | 1.9 |
| 44SDS047 | 2.562 | 2.575 | 2.611 | 2.716 | 2.711 | 2.2 | 1.9 | 1.4 |
| 45B2W078 | 2.760 | 2.724 | 2.653 | 2.808 | 2.798 | 0.6 | 1.0 | 2.0 |
| 45B2W078 | 2.691 | 2.692 | 2.642 | 2.777 | 2.796 | 1.1 | 1.4 | 2.1 |
| 45DGG114 | 2.654 | 2.658 | 2.639 | 2.713 | 2.711 | 0.8 | 0.7 | 1.0 |
| 45DGG115 | 2.627 | 2.647 | 2.662 | 2.716 | 2.723 | 1.3 | 1.1 | 0.8 |
| 45JDR206 | 2.431 | 2.412 | 2.444 | 2.609 | 2.615 | 2.8 | 3.2 | 2.7 |
| 45JDR225 | 2.429 | 2.479 | 2.545 | 2.602 | 2.637 | 2.7 | 2.4 | 1.4 |
| 45JDR225 | 2.754 | 2.526 | 2.458 | 2.812 | 2.619 | 0.8 | 1.4 | 2.5 |
| 45TMS137 | 2.627 | 2.666 | 2.644 | 2.690 | 2.729 | 0.9 | 0.9 | 1.2 |
| 45TMS137 | 2.624 | 2.635 | 2.644 | 2.731 | 2.729 | 1.5 | 1.3 | 1.2 |
| 45TMS137 | 2.681 | 2.654 | 2.604 | 2.742 | 2.726 | 0.8 | 1.0 | 1.7 |
| 45TMS155 | 2.635 | 2.616 | 2.586 | 2.731 | 2.718 | 1.3 | 1.4 | 1.9 |
| 45TMS156 | 2.625 | 2.631 | 2.626 | 2.734 | 2.735 | 1.5 | 1.4 | 1.5 |
| 45TMS163 | 2.735 | 2.651 | 2.629 | 2.807 | 2.714 | 0.9 | 0.9 | 1.2 |
| 45TMS163 | 2.599 | 2.626 | 2.630 | 2.698 | 2.714 | 1.4 | 1.2 | 1.2 |
| 45TMS174 | 2.617 | 2.729 | 2.644 | 2.651 | 2.806 | 0.5 | 1.0 | 2.2 |
| 45TMS174 | 2.613 | 2.625 | 2.644 | 2.797 | 2.806 | 2.5 | 2.5 | 2.2 |
| 45TMS175 | 2.617 | 2.710 | 2.620 | 2.651 | 2.794 | 0.5 | 1.1 | 2.4 |
| 45TMS175 | 2.608 | 2.613 | 2.621 | 2.782 | 2.794 | 2.4 | 2.5 | 2.4 |
| 45TMS176 | 2.563 | 2.617 | 2.651 | 2.802 | 2.803 | 2.7 | 2.5 | 2.0 |
| 45TMS176 | 2.678 | 2.726 | 2.651 | 2.720 | 2.803 | 0.6 | 1.0 | 2.0 |
| 46LRB066 | 2.565 | 2.568 | 2.577 | 2.703 | 2.706 | 2.0 | 2.0 | 1.9 |
| 48MA0039 | 2.522 | 2.523 | 2.547 | 2.645 | 2.631 | 1.8 | 1.6 | 1.3 |
| 48MA0105 | 2.695 | 2.613 | 2.608 | 2.741 | 2.644 | 0.6 | 0.4 | 0.5 |
| 48MA0105 | 2.579 | 2.607 | 2.607 | 2.626 | 2.644 | 0.7 | 0.5 | 0.5 |
| 48MA0108 | 2.577 | 2.590 | 2.599 | 2.690 | 2.692 | 1.6 | 1.5 | 1.3 |
| 48MA0108 | 2.617 | 2.647 | 2.599 | 2.651 | 2.692 | 0.5 | 0.6 | 1.3 |
| 48MA0109 | 2.617 | 2.641 | 2.566 | 2.651 | 2.706 | 0.5 | 0.9 | 2.0 |
| 48MA0109 | 2.596 | 2.584 | 2.566 | 2.705 | 2.706 | 1.6 | 1.7 | 2.0 |
| 49KVT080 | 2.579 | 2.594 | 2.635 | 2.791 | 2.792 | 2.9 | 2.7 | 2.1 |
| 49KVT081 | 2.597 | 2.591 | 2.629 | 2.798 | 2.783 | 2.8 | 2.7 | 2.1 |
| 49KVT081 | 2.527 | 2.550 | 2.645 | 2.795 | 2.790 | 3.8 | 3.4 | 2.0 |
| 54SDS080 | 3.534 | 3.577 | 3.594 | 3.695 | 3.821 | 1.2 | 1.8 | 1.7 |
| 54SDS081 | 3.534 | 3.451 | 3.433 | 3.695 | 3.699 | 1.2 | 1.9 | 2.1 |
| 55J2D008(C3) | 2.628 | 2.626 | 2.609 | 2.655 | 2.648 | 0.4 | 0.3 | 0.6 |
| 55TMS029(C1) | 2.650 | 2.646 | 2.625 | 2.775 | 2.781 | 1.7 | 1.8 | 2.1 |
| 55TMS030(C2) | 2.639 | 2.637 | 2.639 | 2.788 | 2.785 | 2.0 | 2.0 | 2.0 |
| 57R7S215(A1) | 2.538 | 2.524 | 2.559 | 2.766 | 2.779 | 3.2 | 3.6 | 3.1 |
| 57R7S216(A2) | 2.581 | 2.571 | 2.611 | 2.798 | 2.787 | 3.0 | 3.0 | 2.4 |
| 57R7S217(A4) | 2.584 | 2.582 | 2.621 | 2.797 | 2.791 | 3.0 | 2.9 | 2.3 |
| 57R7S218(A3) | 2.584 | 2.572 | 2.604 | 2.797 | 2.792 | 3.0 | 3.1 | 2.6 |
| 69WPM070 | 2.927 | 2.911 | 2.857 | 2.982 | 2.982 | 0.6 | 0.8 | 1.5 |
| 69WPM074 | 2.927 | 2.917 | 2.859 | 2.982 | 2.993 | 0.6 | 0.9 | 1.6 |
| J5I0679 | 2.570 | 2.588 | 2.587 | 2.670 | 2.687 | 1.5 | 1.4 | 1.4 |
| J5P0704 | 2.631 | 2.627 | 2.611 | 2.718 | 2.711 | 1.2 | 1.2 | 1.4 |
| J5P0704 | 2.631 | 2.632 | 2.617 | 2.718 | 2.715 | 1.2 | 1.2 | 1.4 |
| J6U1047 | 2.610 | 2.598 | 2.609 | 2.737 | 2.725 | 1.9 | 1.8 | 1.6 |